

Electronic Theses and Dissertations, 2004-2019

2009

Formation Of Lyotropic Liquid Crystals Through The Self-assembly Of Bile Acid Building Blocks

Karan Tamhane
University of Central Florida

 Part of the [Materials Science and Engineering Commons](#)
Find similar works at: <https://stars.library.ucf.edu/etd>
University of Central Florida Libraries <http://library.ucf.edu>

This Masters Thesis (Open Access) is brought to you for free and open access by STARS. It has been accepted for inclusion in Electronic Theses and Dissertations, 2004-2019 by an authorized administrator of STARS. For more information, please contact STARS@ucf.edu.

STARS Citation

Tamhane, Karan, "Formation Of Lyotropic Liquid Crystals Through The Self-assembly Of Bile Acid Building Blocks" (2009). *Electronic Theses and Dissertations, 2004-2019*. 4093.
<https://stars.library.ucf.edu/etd/4093>



FORMATION OF LYOTROPIC LIQUID CRYSTALS THROUGH THE SELF-ASSEMBLY OF BILE ACID BUILDING BLOCKS

by

KARAN TAMHANE
B.E. University of Pune, 2007

A thesis submitted in partial fulfillment of the requirements
for the degree of Master of Science
in the Department of Mechanical, Materials and Aerospace Engineering
in the College of Engineering and Computer Science
at the University of Central Florida
Orlando, Florida

Fall Term 2009

© 2009 Karan Tamhane

ABSTRACT

Liquid crystalline materials (LCMs) have gained much popularity over the past century. The thermotropic forms of these materials have been extensively studied and employed in a range of innovative applications. The lyotropic liquid crystal systems that have been studied in the past have often been formed by the organization of natural and synthetic small molecules in solutions.

In this study, we use self-assembled supramolecular structures as building blocks to fabricate lyotropic liquid crystals. We investigate the self-assembly of a naturally occurring bile acid called lithocholic acid (LCA), to form supramolecular fibrous and tubular structures in basic aqueous solutions. We control the morphology of the self-assembled structures by manipulating experimental parameters in order to gain comprehensive knowledge regarding the self-assembly process. We characterize these structures with respect to their morphology i.e. their length, diameter, flexibility and shape using atomic force microscopy, optical microscopy and infrared spectroscopy.

We produce lyotropic liquid crystal phases using self-assembled LCA structures through modification of physical parameters such as concentration, temperature, shear and pH. The nature of the lyotropic liquid crystal phases depends upon the morphology of the fibers and tubes. We observe that the short, rigid fibers and tubes form nematic phases while long, flexible fibers and tubes form cholesteric phases. We also study the phase transitions of the liquid crystal (LC) phases by observing their patterns using a polarizing microscope. Observations show that LC phases form in samples with LCA concentration above 0.75%w/w. Since the process of self-assembly is time-dependent,

so is the formation of liquid crystal phases. We note that the optimum LCA concentration for LC phase formation is 2%-4%w/w and that the liquid crystal transition temperature is about 70°C.

I would like to dedicate this thesis to my parents, my family and all my friends who have always stood by me in all walks of life. I owe them my heartfelt gratitude for their unwavering support and good wishes.

ACKNOWLEDGEMENTS

I would like to take this opportunity to sincerely thank my advisor Dr. Jiyu Fang for helping me learn and for guiding me throughout my stay at UCF. He has been very supportive and I owe him all my knowledge of research methods and data analysis among other things. He has taught me to be persistent in everything I do and has set an excellent example of hard work and diligence.

I am grateful to Dr. Hyoung Jin Cho and Dr. Andre Gesquiere for being part of my thesis committee and helping me to raise the quality of my work. Their contribution is invaluable.

I would also like to thank Dr. Xuejun Zhang for her invaluable help in all my endeavors and her enjoyable company at work. I am glad to have had her as my colleague and appreciate all her support and encouragement.

I thank Dr. Yue Zhao for teaching me important characterization tools and data analysis methods and for helping me out in my work without hesitation.

I also thank Fred Kobzeff and Rong Fan for being friendly and supportive colleagues and making work fun.

I am indebted to all the people who have helped me during my stay at UCF, especially the faculty members, Dr. Jianhua, Amit, Ajay, Mahadevan, Abhilash, and Zeyu.

Last but not the least; I profusely thank my roommates and all my friends who made life enjoyable in an unknown country.

TABLE OF CONTENTS

LIST OF FIGURES.....	ix
CHAPTER 1: INTRODUCTION.....	1
1.1 Classification of Liquid Crystalline Materials	4
1.1.1 Thermotropic Liquid Crystals	4
1.1.2 Lyotropic Liquid Crystals:.....	8
1.2 Liquid Crystals and Self-assembly	11
1.2.1 What is Self-assembly?	11
1.2.2 Applications of Self-assembly	12
1.3 Focus of Research.....	13
CHAPTER 2: SYNTHESIS AND CHARACTERIZATION OF SELF-ASSEMBLED BILE ACID TUBES AND FIBERS	15
2.1 The Self-Assembling Molecule.....	15
2.2 Synthesis and Properties of Coiled Sodium Lithocholate Tubes and Fibers....	17
2.2.1 Experimental Method.....	17
2.2.2 Results and Discussion.....	17
2.3 Synthesis and Properties of Straight Sodium Lithocholate Tubes and Fibers.	33
2.3.1 Experimental Method	33
2.3.2 Results and Discussion.....	34
2.3.3 Mechanical Properties of Different Tubes	41
2.4 Synthesis and Properties of LCA Fibers Using Organic Bases.....	44

2.4.1	Structure of Organic Bases Employed	44
2.4.2	Experimental Method	45
2.4.3	Results and Discussion.....	46
CHAPTER 3: FORMATION OF LIQUID CRYSTALS		51
3.1	Mechanism of Formation of Liquid Crystals	51
3.2	Concentration-induced Liquid Crystal formation in Open Cells	52
3.2.1	Experimental Method	53
3.2.2	Results and Discussion.....	53
3.3	Temperature-induced Liquid Crystal formation in Closed Cells	63
3.3.1	Plain Glass Cells.....	63
3.3.2	Glass Cells Coated with Polyimide Layer	67
3.3.3	Liquid Crystals in a Channel	68
3.4	Formation of LC Phases from EA and EDA samples.....	70
3.4.1	LCA with Ethylamine.....	70
3.4.2	LCA with Ethylenediamine	71
CHAPTER 4: CONCLUSION		73
LIST OF REFERENCES		76

LIST OF FIGURES

Figure 1.1 - Comparison of LCs to solids and liquids	2
Figure 1.2 - Variation of order parameter (S) with temperature.....	4
Figure 1.3 - Types of simple thermotropic mesophases (a) Nematic (b) Smectic A (c) Smectic C.....	5
Figure 1.4 - (a) Chiral nematic phase (b) Chiral smecticC phase.....	7
Figure 2.1 - Structure of Lithocholic Acid.....	16
Figure 2.2 - (a) Crystalline arrangement of fibers induced by NaOH. (b) Colorful birefringence on account of random arrangement of fibers.....	19
Figure 2.3 - Atomic Force Microscope image of packed fibers scanned after drying	20
Figure 2.4 - Aggregates seen in the diluted sample (a) Bright field image (b) Image under cross polarizer.....	21
Figure 2.5 - AFM images of (a) Rod-shaped fiber aggregates (b) Star-shaped secondary aggregates (c) Cross-section view of star branches [taken at dotted line in (b)]	22
Figure 2.6 - Coiled tubes formed at high pH (a) segmental structure of tubes (b) aggregation of randomly coiled tubes (c) & (d) dark field images of the sample.	23
Figure 2.7 - Hollow structure of the self-assembled structures.....	24
Figure 2.8 - LCA concentration change in the lower range. (a) 0.075% (b) 0.15% (c) 0.2% (d) 0.25%	25
Figure 2.9 - Change in morphology with respect to LCA concentration (a) Effect on aggregate size (b) Effect on aggregate number	27

Figure 2.10 - Samples with high concentration of LCA (a) bright field image (b) dark field image	28
Figure 2.11 - Effect of NaOH concentration on morphology (a) 0.05M (b) 0.075M (c) 0.1M (d) 0.15M.....	29
Figure 2.12 - Change in morphology of aggregates with different NaOH solution strength (a) 0.8M (b) 0.5M (c) 0.4M (d) 0.3M (e) 0.2M.....	30
Figure 2.13 - Sample with 0.25% LCA and 0.1M NaOH broken down on sonication	31
Figure 2.14 - Sonication after addition of water.....	32
Figure 2.15 - Formation of dense gels through thermal processing (a) Before heating (b) After heating.....	33
Figure 2.16 -Aggregation in samples made at low pH values	35
Figure 2.17 - Progression of growth of self-assembled aggregated structures at pH 7 (a) rod-like initial aggregates (b) star-like secondary aggregates (c) star-shaped aggregates grow and branches become thin (d) branches grow long enough to become flexible and bend.	36
Figure 2.18 -Birefringent patterns shown by aggregates (a) Optical image and (b) Corresponding dark field image	37
Figure 2.19 - AFM image of a straight fiber	37
Figure 2.20 -Broken down fibers after sonication	38
Figure 2.21 - Length distribution of sonicated straight fibers	39
Figure 2.22 - Effect of sodium chloride on the morphology of straight rods and tubes (a) original sample (b) 7.5mg/ml NaCl (c) 25mg/ml NaCl (d) 100mg/ml NaCl	40

Figure 2.23 – Assessment of mechanical properties using the cutting method (a) Curved tube and (b) Straight tube	41
Figure 2.24 - FTIR scans of coiled and straight tubes	43
Figure 2.25 - Ethylamine	45
Figure 2.26 – Ethylenediamine.....	45
Figure 2.27 - EDA sample (a) Individual fibers/tubes on day 2 (b) Aggregation on day 5	47
Figure 2.28 - EDA sample 6 months post synthesis.....	47
Figure 2.29 - AFM images of EDA sample (a) Showing fiber structure (b) Layered growth of fibers.....	48
Figure 2.30 - EA sample (a) Individual fibers/tubes (b) Aggregation (c) & (d) AFM images	49
Figure 2.31 - FTIR studies of 0.1% w/w LCA samples with 0.1M EDA and EA.....	50
Figure 3.1 - Cross sectional view of an open cell	52
Figure 3.2 - Stepwise heating of 4% LCA sample in open cell	55
Figure 3.3 - Cooling of 4% LCA sample in open cell (from Fig. 3.2).....	55
Figure 3.4 - Growth of coarse LC domains with time (from Fig. 3.3).....	56
Figure 3.5 - Formation of fine domains through direct heating of 3% LCA sample on cooling.....	57
Figure 3.6 - 3% LCA sample (a) Dark field image when cooled after direct heating (b) Corresponding bright field image (c) Growth of domains with time	57
Figure 3.7 - Change in optical pattern with respect to LCA concentration.....	58

Figure 3.8 - Temporal progress of 1% w/w LCA sample with respect to LC formation (a) Day1.....	59
Figure 3.9 - Evaporation induced LC formation (a) Initial stage (b) Ordering at the edge (c) Growth of domains with time.....	60
Figure 3.10 - 2% w/w LCA sample at near neutral pH.....	62
Figure 3.11 – Cross sectional view of a closed cell.....	63
Figure 3.12 - 3% w/w LCA sample in a closed cell.....	64
Figure 3.13 - Cholesteric LC phase in 3% w/w LCA sample	65
Figure 3.14 - Image showing fiber arrangement in 3% w/w LCA sample	66
Figure 3.15 - LC alignment in polymer coated cells with respect to cell thickness (a) 5 μ m (b) 8 μ m (c) 10 μ m (d) 12 μ m (e) 15 μ m.....	67
Figure 3.16 - Liquid Crystal formation in a microchannel	68
Figure 3.17 – 2% w/w sample (a) & (b) Disorder before heating (c) to (f) Ordering during cooling.....	69
Figure 3.18 - Nematic phase observed in the channel (clockwise rotation).....	69
Figure 3.19 - Rings formed in the channel due to flow	70
Figure 3.20 - 2% w/w LCA in EA solution (a) 40°C (b) 50°C (c) 60°C (d) 65°C.....	71
Figure 3.21 - 2% w/w LCA in EDA solution (a) 40°C (b) 50°C (c) 60°C (d) 65°C	71
Figure 3.22 - Formation of LC phase in EDA sample.....	72
Figure 3.23 - 2% LCA with EDA sample after 2 hours (a) Bright field image (b) Dark field image	72

CHAPTER 1: INTRODUCTION

Recent times have seen a tremendous increase in the use of nano- and micro-scaled materials in technological applications in various fields of science ^[1-4]. Biological systems have been studied for centuries in order to learn the secrets of nature. Natural systems possess molecular precision, immaculate design, perfect symmetry and exceptional functionality which are undoubtedly also desirable in artificial devices and hence the field of biomimetics has gained much importance as well ^[5]. A quite fundamental yet extraordinary biological process is that of self-assembly or self-organization ^[6-8]. It is the spontaneous and reversible organization of individual components of a system into ordered structures without external influence. Self-assembly occurs on molecular level as well as meso and macroscopic levels ^[9-10]. An important step in biological self-assembly of organisms is the formation of liquid crystalline cell membranes ^[11]. Liquid crystals are an important class of materials and have been dealt with in the following sections in greater detail.

Thermodynamic systems always try to attain a state of maximum entropy with minimum possible energy. It's this balance of two opposing forces that decides the extent of order or disorder in a system. Solid materials usually possess ordered structures and their molecules display positional and directional order. Positional order refers to the uniform arrangement of molecules or building blocks such that their positions are periodic in space. Directional order refers to the arrangement of molecules or building blocks such that their anisotropic axes are oriented in the same direction in space. On the other hand, molecules that make up a liquid are distributed randomly

throughout its bulk and possess neither positional nor directional order. Liquid crystalline materials are materials which exhibit ordering characteristics intermediate to those of solids and liquids. They usually exhibit directional order and sometimes both, directional and positional order. Liquid crystalline materials (LCMs) contain molecules that are ordered and mobile at the same time. These materials were first observed by Friedrich Reinitzer^[12] and Otto Lehmann^[13] during the end of the 19th century. Reinitzer knew Lehmann was an expert in polarized microscopy and wanted him to take a look at an unusual sample he had come across. Lehmann describes thoroughly, the experiments carried out to examine the above said sample which was actually the compound cholesteryl benzoate. Later George Freidel^[14] classified liquid crystalline materials into different types viz. nematic, smectic, cholesteric, etc.

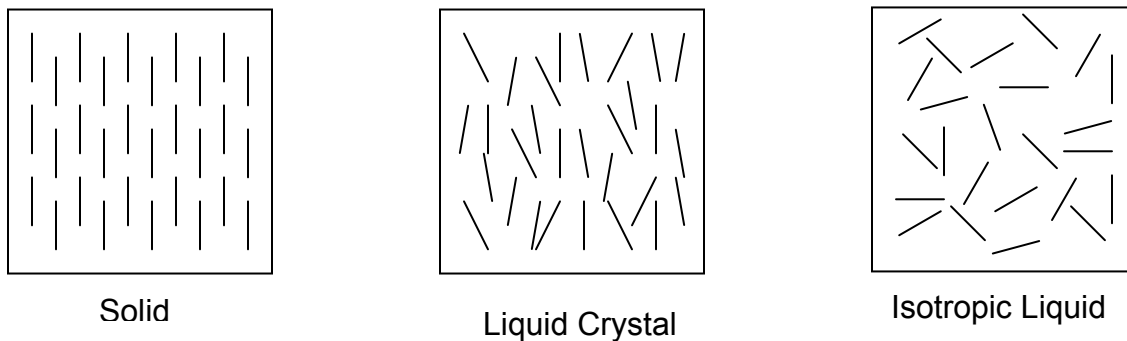


Figure 1.1 - Comparison of LCs to solids and liquids

It is clear from Fig. 1.1^[15] how materials differ in their molecular ordering in bulk phase. The degree of order decreases from solids to LCMs to liquids. LCMs are also called mesomorphic materials and the extent of ordering behavior that they exhibit is much lesser than that in crystals (solids). The latent heat values for the crystal-liquid transition are around 250 J/g while those for the liquid crystal-liquid transition are only about 5 J/g^[16]. The unit vector in the preferred direction of orientation of liquid

crystalline molecules in called the director. The molecules in a mesomorphic material are oriented such that they point more or less in the direction of the director and thus establish orientational order in the system.

The degree of order in different mesophases is characterized by a variable called the order parameter 'S' ^[17] which is defined as

$$S = \langle P_2 \langle \cos^2 \theta \rangle \rangle = \langle \frac{3}{2} \cos^2 \theta - \frac{1}{2} \rangle$$

Here θ is the angle made by the molecular axis with the director. The value of S is taken as an average over θ values of all the molecules at one instant. Another method to calculate the value of S is to take an average over all θ values of one molecule observed over a long period of time. The value of the order parameter varies from zero for a completely disordered mesomorphic system, to one for an ordered system. The temperature above which a liquid crystalline system transitions to a completely disordered system (liquid) is called the critical transition temperature T_C . The variation of S with respect to T is shown in Fig 1.2 below. It is seen that the order parameter decreases with increasing temperature and goes down to zero at $T = T_C$.

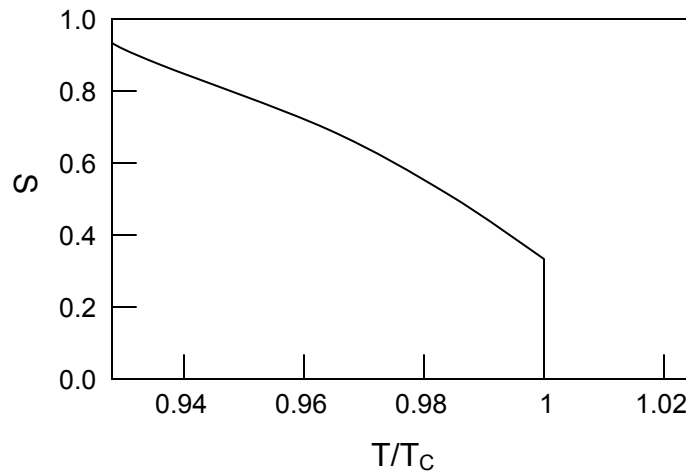


Figure 1.2 - Variation of order parameter (S) with temperature

1.1 Classification of Liquid Crystalline Materials

1.1.1 Thermotropic Liquid Crystals

As the name suggests, thermotropic liquid crystals are formed due to the effect of heat. When a solid is heated, it transforms into a mesophase at a temperature lower than its melting temperature. This temperature is called the critical temperature T_c . In 1888, Reinitzer observed that some organic compounds on heating undergo two distinct thermal transitions instead of one (i.e. melting). He found this to be quite prominent in a compound called cholesteryl benzoate that he was studying. When this compound was heated, it first melted into a cloudy liquid which on further heating turned clear. The first transition that was observed was attributed to an intermediate phase that showed fluidity but showed ordering as well. Due to the crystalline nature of this phase, it was opaque. This cloudy phase that was observed later came to be called as the cholesteric

or chiral nematic LC phase. Thermotropic liquid crystals are thus stable over a certain temperature range ^{[16] [18]}. They can be made up of either rod-shaped or disc-shaped mesogens. The mesophases formed from the former are called calamitic mesophases while those formed from the latter are called discotic mesophases. The main types of calamitic liquid crystalline phases are the nematic and smectic phases, both of which are explained in greater detail in the following section. Discotic thermotropic liquid crystals exhibit nematic and columnar phases.

1.1.1.1 Liquid Crystal Phases

Nematic liquid crystals

These are the simplest type of liquid crystalline materials. The molecules possess orientational order but no positional order in a nematic liquid crystal Fig. 1.3 shows the different liquid crystalline phases.

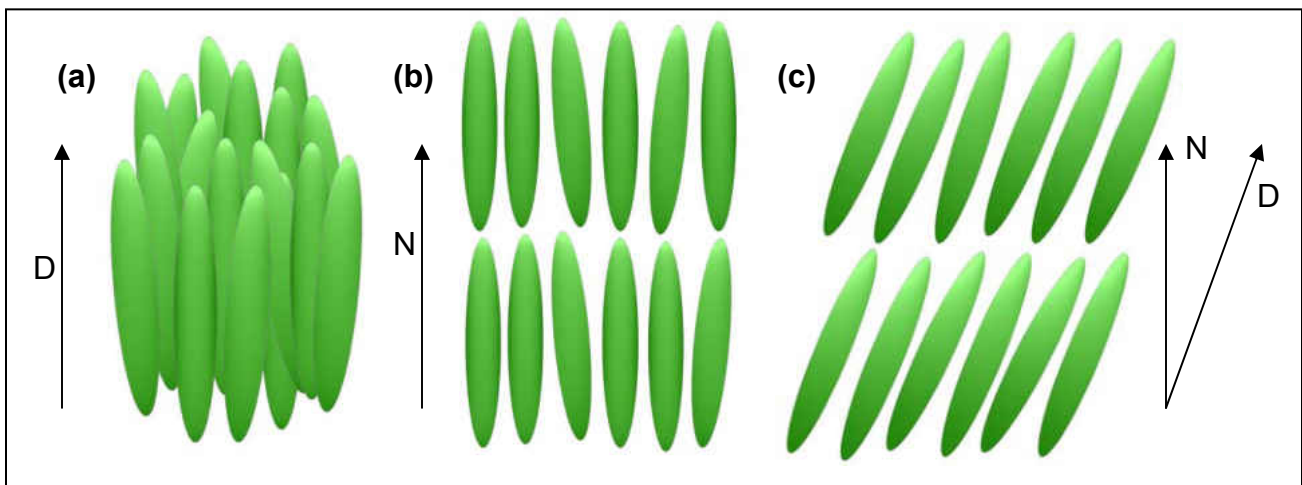


Figure 1.3 - Types of simple thermotropic mesophases (a) Nematic (b) Smectic A (c) Smectic C

Smectic liquid crystals

There are two types of smectic mesophases, smectic A and smectic C. Both these mesophases possess positional as well as directional order as they exist at lower temperatures compared to the nematic mesophase. At lower temperatures, thermal vibrations of the molecules reduce, facilitating better ordering. Smectic phases possess layered structures and the orientation of molecules in these layers determines the type of the smectic phase. In the smectic A mesophase the molecules are oriented such that the normal to the layer is parallel to the director [Fig. 1.3 (b)]. In the smectic C phase, the director lies at an angle to the layer normal [Fig. 1.3 (c)].

Chiral liquid crystal phases

The chiral nematic and the chiral smectic C mesophases are included in this class of LCMs. The mesogens in these phases possess chirality which results in a gradual change in the orientation of the director from one layer of mesogens to the other. In both, the chiral nematic and chiral smectic C phases, this rotation of the director leads to the formation of helical assemblies of the mesogens. Nematic phases can be converted into chiral nematic phases by addition of a small amount of chiral (optically active) dopant ^[19]. These mesophases are birefringent on account of the existent chirality. Fig 1.4 shows the chiral mesophases and the helical arrangements present in them.

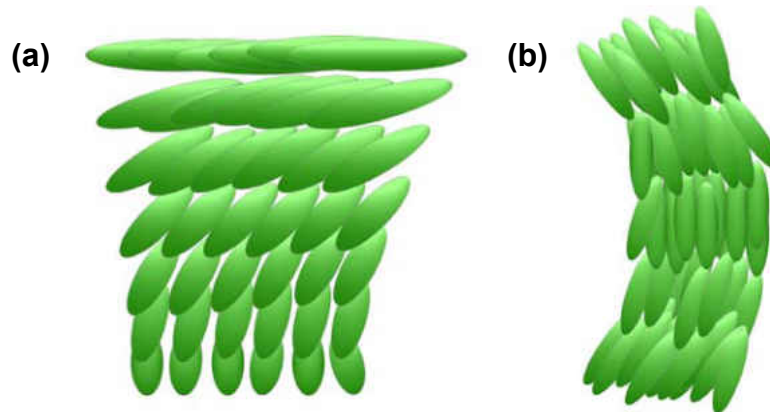


Figure 1.4 - (a) Chiral nematic phase (b) Chiral smectic C phase

1.1.1.2 Applications of Thermotropic Liquid Crystals

Liquid crystalline materials have been used for a variety of applications, the most well known of them being liquid crystalline displays (LCDs). These applications are discussed in this section in order to exemplify the importance of LCMs.

Liquid Crystal Displays

LCDs ^[20] are flat cells containing nematic or smectic C materials that are electro-responsive i.e. they respond to voltage changes. Some displays can be made out of polymer liquid crystals as well.

Spatial Light Modulators

Liquid crystalline films or thin cells can be used as modulators on account of their optical properties. A device that controls transmittance is called a light valve and a device that controls transmittance independently at different positions in space is a spatial light modulator ^[20]. They are used in overhead LCD projectors.

Thermometers

Strips of thermochromic LCMs are used as thermometers since they can display different colors corresponding to different temperatures ^[21].

1.1.2 Lyotropic Liquid Crystals:

Lyotropic LCMs are ones which exhibit ordered mesophases in solutions rather than in their pure form. Thus these LCMs are made of two or more components ^[22], the solvent usually being water ^[23]. The formation of the mesophase depends on the concentration of the mesomorphic material in the solution as well as its temperature. The kinds of molecules that make up the lyotropic liquid crystal system are called amphiphilic molecules. They are mostly hydrophobic organic molecules with a hydrophilic head group that gives them a dual nature. When these materials are added to a solvent, they dissolve like any other solute till the concentration reaches a particular level. At this concentration, the molecules gather together in order to reduce the energy of the system. At this concentration level, the molecules form clusters throughout the solution and this particular concentration is called the critical micelle concentration. The shape and size of these clusters depends on the type and concentration of the molecules ^[24]. For example soap molecules form different phases in aqueous solutions. At very low concentrations, the soap forms a true solution i.e. all molecules are totally solvated. At the critical micelle concentration, soap molecules form micelles and the size and number of these micelles increases with increasing concentration. At higher concentrations, the micelles become rod-shaped and begin arranging in an ordered fashion. This is one of the liquid crystalline phases of soap. If the concentration is

increased even more, the molecules form bilayer sheets with the hydrophilic head groups pointing outwards and hydrophobic tails encased within. These bilayers are similar to the smectic mesophases observed in thermotropic liquid crystals. If the concentration is high enough and if other conditions are met, the bilayers can fold or twist to form tubular structures. We shall talk about the formation of such structures in subsequent sections of the manuscript.

1.1.2.1 Lyotropic Liquid Crystal Phases

As already discussed, amphiphilic molecules form circular or rod-shaped micelles (or reverse micelles) in aqueous solutions. The rod-shaped micelles usually form the hexagonal lyotropic liquid crystal phase in which the micelles are arranged in a hexagonal pattern in the solution. A reverse hexagonal arrangement is also possible but it is much rarely seen. These phases are highly viscous on account of high concentration of LC molecules. Circular micelles, on the other hand, form cubic lyotropic liquid crystals which are not too frequently seen. The cubic arrangement can be discontinuous (like atoms arranged at the corners of a cube) or bicontinuous (with either the LC molecules or water making a network in the interior of the cube). Cubic phases are even more viscous as compared to hexagonal phases due to absence of shear planes. At very high concentrations, typically a lamellar lyotropic liquid crystalline phase is observed. In this phase the molecules form sets of two parallel sheets with water sandwiched between them. The sheets are arranged such that the hydrophobic tails of molecules in adjacent sheets point toward each other. The water layers are sandwiched between two sheets with the polar head groups pointing toward the water.

The lamellar bilayer phase is the least viscous in spite of having a high concentration of the amphiphiles since sliding of sheets is relatively easy under shear.

In addition to these phases, lyotropic liquid crystals also form nematic and cholesteric phases ^[25]. Solutions with disc-like micelles form lamellar nematics while those with rod-like micelles form cylinder nematics. Both these nematic phases can change into the biaxial nematic phase due to a change in either concentration or temperature or both. The biaxial phase usually exists between the lamellar and cylinder nematic phases. If the molecules possess chirality or if a chiral dopant is added to the solution, the corresponding cholesteric phases are obtained.

1.1.2.2 Importance of Lyotropic Liquid Crystals in Life

Lyotropic liquid crystals play an extremely important role in the biological world ^[26]. Organisms must have an efficient way of exchanging materials between their cells. The cells need to have a sound structure as well as an ability to facilitate this exchange. Both these functions cannot be accomplished on their own either by solids or liquids. Thus there is a necessity for a phase which has properties intermediate to those of solids and liquids. Lyotropic liquid crystals meet these requirements and provide structural integrity as well as a means for the transport of materials. Lyotropic liquid crystals are easy to form in living organisms as they are all made up of water-based cells. The first observation of biological liquid crystalline materials was made in 1850 when a birefringent pattern was obtained from myelin (an insulating material made out of lipids and proteins) present on the nerve cells ^[27]. The cellular membranes of living organisms are mostly made up of phospholipids which form liquid crystalline phases in

aqueous solutions. Different types of organisms have different liquid crystalline systems which govern their bodily functions. The transition temperatures of these systems depend on the environment in which the organism lives. If the ambient temperature reduces well below the LC transition temperature, the organism is likely to die. It is clear that although thermotropic liquid crystals are more widely known, lyotropic liquid crystalline materials are much more important, in that they are crucial for the creation and sustenance of life.

1.2 Liquid Crystals and Self-assembly

As previously seen, liquid crystalline materials consist of mesogens which are associated with a certain degree of order. Self-assembly and liquid crystalline transition are somewhat similar processes in that both involve the rearrangement of molecules (or building units) in order to achieve a state of equilibrium. Also both these phenomena involve non-covalent interactive forces. If these processes were to be used in tandem with each other, it could be possible to synthesize liquid crystalline materials through self-assembly^[28].

1.2.1 What is Self-assembly?

Self-assembly is the spontaneous organization of building blocks into ordered structures without any external influence. In our study, we shall refer to self-assembly of chemical units like molecules and some molecular aggregates. During self-assembly, the molecules organize through non-covalent interactions like dipole moments, Van der Waals forces, hydrogen bonds etc.^[29-31]. All biological assemblies are created through

the process of self-assembly or self-organization. We ourselves are products of the process of self-assembly! It is thus extremely important to study and understand self-assembly if we hope to understand the origin of life.

Since the components of the system are arranged through secondary bonding, the assembly can be broken down by changing certain system parameters. Thus, the process is a reversible one and can occur only under certain defined conditions ^[9]. If there is a deviation from these conditions, the system goes back to its disordered state. It is possible to obtain desired supramolecular structures through self-assembly by designing the initial building blocks or components as well as controlling the reaction conditions. Molecules can be chemically tailored to meet specific requirements of a particular desired arrangement by use of proper synthetic methods. The final structure of the supramolecular system depends upon the nature and extent of the intermolecular forces of attraction present. Amphiphilic molecules have been seen to form ribbons, tubes and fibers through self-organization ^[32-40].

1.2.2 Applications of Self-assembly

A few examples of the applications of self-assembly are listed below in order to explain its significance as a synthetic process.

1.2.2.1 Synthesis of nanomaterials through the bottom-up approach

The top-down approach cannot be used to synthesize nanostructures in all scenarios ^[v]. Moreover, self-assembly is a process that does not require any external energy or control and desired nanostructures form spontaneously. Hence it is an

important synthetic method to produce large functional assemblies of fundamental structural units^[41].

1.2.2.2 Tissue Engineering and Cell Culture

Self-assembly is the process by which living cells organize into complex structures. It is possible to use this same process to produce artificial or synthetic tissues for biomedical applications like prosthetics, grafts, etc.

1.3 Focus of Research

In this study we investigate the formation of liquid crystalline phases from self-assembled mesogens. The mesogens are fibers of self-assembled bile acid molecules in aqueous basic solutions. We begin by studying the process of formation of the self-assembled fibers and their aggregation properties to assess their ordering nature. We study different systems with respect to different reaction parameters and environments. The particular bile acid under study was lithocholic acid (LCA). A more detailed discussion about the structure and properties of LCA will be done in subsequent chapters.

Not a lot of work has been carried out in the formation of liquid crystals using supramolecular structures as mesogens. Work has been done on other biological molecules like DNA^[42-46] and RNA^{[44][47]}, but these molecules are naturally occurring complex molecules and it is hard to change their structure and morphology. The only parameter that is easiest to change is the length of the molecules. In this study, however, the mesogens that make up the liquid crystalline phase are unique in that they

are not individual molecules that orient to form the mesophase. Each mesogen is a collection of molecules which is held together by weak attractive forces. An advantage of these kinds of mesogens is that they can change the structure of the mesophase with a change in the self-assembled structure. For example, a thermotropic folic acid derivative changes from smectic phase to hexagonal columnar phase by the addition of alkali metal salts ^[48]. Another important thing about this study is that it uses lithocholic acid which is a bile acid found in the bodies of mammals. Thus, we use naturally available biological molecules to make mesogens through the natural process of self-assembly. The nature of the self-assembled structures can be manipulated by changing their environmental conditions. We study the effect of various parameters on the self-assembled structures.

The self-assembled structures can be organized to form liquid crystalline phases of different kinds. The nature of the phases naturally depends upon the characteristics of the self-assembled structures. We study the changes in the LC phases as a function of different experimental parameters resulting and consequently, different supramolecular structures.

CHAPTER 2: SYNTHESIS AND CHARACTERIZATION OF SELF-ASSEMBLED BILE ACID TUBES AND FIBERS

In this chapter, we talk about the molecule we use to form self-assembled fibers. We also discuss the process of bile acid self-assembly and the different structures that are formed. We look at the effects of changes in experimental parameters and environments on the tubes and fibers and their structures.

2.1 The Self-Assembling Molecule

Lithocholic acid is a bile acid found in the bodies of humans. Bile acids are formed in the liver by oxidation of cholesterol and are stored in the gallbladder ^[49-50]. They are normally conjugated with taurine, glycine, sulfates or glucuronides and this increases their water solubility. They solubilize fats and fat soluble vitamins ^[51] and help in breaking them down in the intestine. Lithocholic acid is one of the rarer bile acids in that it is found in smaller quantities in the human body than the other bile acids. Lithocholic acid is a liver-toxic material and hence it is necessary for its sulfation to take place. The human body effectively sulfates lithocholic acid and hence it is not harmful unless a disorder inhibits the sulfation process. It is thus, safe to assume that average human beings are immune to its toxicity and that it can be used in biological applications.

Bile acids and their derivatives display self-association in aqueous solutions ^[52-55] and the chemical structure of each bile acid is responsible for the extent to which it aggregates ^[56]. Due to their unique assembling properties, bile acids and bile salts have gained importance in supramolecular chemistry ^[57-58]. The LCA molecule contains a steroid backbone like all bile acids and ends in a 4 carbon chain containing the carboxyl group. It also has a hydroxyl group on the far end of the molecule as can be seen from the image in Fig. 2.1.

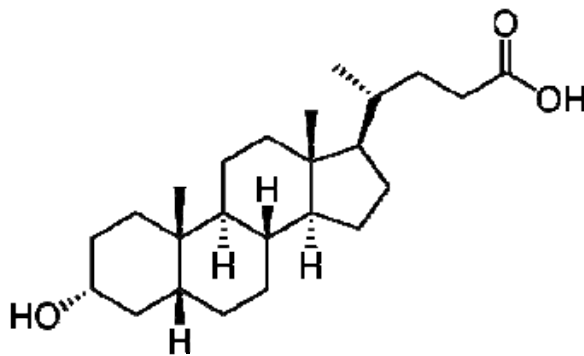


Figure 2.1 - Structure of Lithocholic Acid

The LCA molecule possesses chirality and is thus optically active. The macromolecular assemblies formed from LCA are seen to be crystalline on account of the birefringence displayed. It is seen that these assemblies are also chiral in nature and they are said to possess supramolecular chirality ^[59-60]. LCA can be considered to be an amphiphilic molecule since it has a rigid hydrophobic backbone with two polar groups on opposite ends. The polar groups are not influential enough to balance the hydrophobicity of the molecule, thus rendering it almost insoluble in pure water. It is, however, soluble in aqueous basic solutions as it gets ionized due to deprotonation ^[61].

We use this fact to make LCA solutions and initiate the process of self-assembly. Depending upon the system and the experimental conditions, the structures formed have different properties.

2.2 Synthesis and Properties of Coiled Sodium Lithocholate Tubes and Fibers.

2.2.1 Experimental Method

In order to synthesize self-assembled fibers, a solution of sodium hydroxide having strength of 0.1 M was initially prepared. Then, Lithocholic acid (Aldrich) was added to the solution so as to make a 0.1% w/w LCA solution. The solution was stirred on a vibrator for about a minute and allowed to stand. The solution obtained was a whitish translucent liquid which is a bit more viscous than water. The solution was prepared at room temperature.

2.2.2 Results and Discussion

2.2.2.1 Formation of Fibers

As mentioned in the previous section, the concentration of the NaOH solution used was 0.1M which roughly corresponds to a pH level of about 12 to 13. Under high pH conditions, the lithocholic acid molecules are ionized and thus easily soluble in the aqueous solution. It is proposed that the sodium cations surround the lithocholate anions and act as counterions. Bile acid molecules are known to easily form micelles above the CMC ^[31]. Due to the hydrophobic-hydrophilic interactions, the lithocholate

ions come together to form spherical micelles/vesicles provided that the concentration of LCA is high enough. These spherical micelles join to form bigger rod-like micelles which in turn join to form tubes and/or fibers. At high pH values this process of growth is favored as is explained in subsequent sections of this manuscript. As a result, after a long period of time, the tubes and fibers grow to a large size both longitudinally and diametrically. The exact mechanism for the transformation of the micelles is yet not known but it is speculated that as the number of micelles increases, they prefer to aggregate into bigger structures. As the tubes grow, they form entanglements and aggregate together. The aggregation tendencies of the tubes or fibers depend upon the concentration of LCA, the pH of the solution and the temperature. A detailed explanation of this will follow as we proceed through the document. As the micelles and fibers grow, the solution changes its optical properties. It is common knowledge that the bigger a particle, the more light it scatters and hence, samples with bigger tubes appear opaque while those with smaller ones are translucent. The bigger aggregates that form over a period of time, thus settle down to the bottom of the solution as a white mass. When the self-assembly is still in process, if the supernatant is tested, it is found that shorter tubes are present in it. This suggests that the process is not an instantaneous one and that the micelles are consumed over time similar to a condensation polymerization reaction. Here we can consider individual spherical micelles to be monomer units that join together to form the long chain i.e. the fiber.

2.2.2.2 Morphology of the fibers and tubes

If a droplet of the aforementioned supernatant is allowed to dry on a glass substrate and is observed under a microscope, it is seen that the tubes organize at the edge of the droplet. It is speculated that this arrangement occurs due to the inherent nature of the sodium hydroxide to crystallize on drying i.e. it pushes the tubes to pack together when it crystallizes. The microscope used for these observations was an Olympus BX40 polarizing optical microscope.

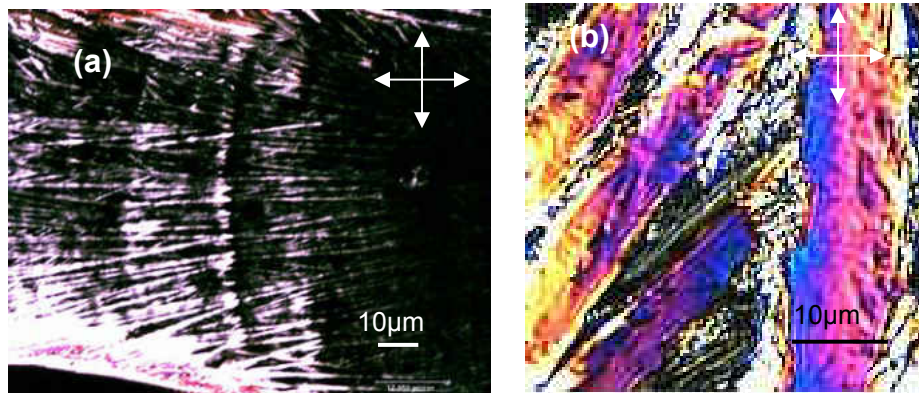


Figure 2.2 - (a) Crystalline arrangement of fibers induced by NaOH. (b) Colorful birefringence on account of random arrangement of fibers.

As seen in the Fig 2.2(a), the tubes form aggregates that arrange in specific long and branched patterns. It was initially thought that the tubes aligned parallel to the longitudinal direction of these branches; but on analyzing the birefringent polarizing microscope pictures [Fig 2.2(b)] and Atomic Force Microscope images, this was found to be untrue. The short tubes were actually seen to be packed in the branches in random fashion [Fig 2.3]

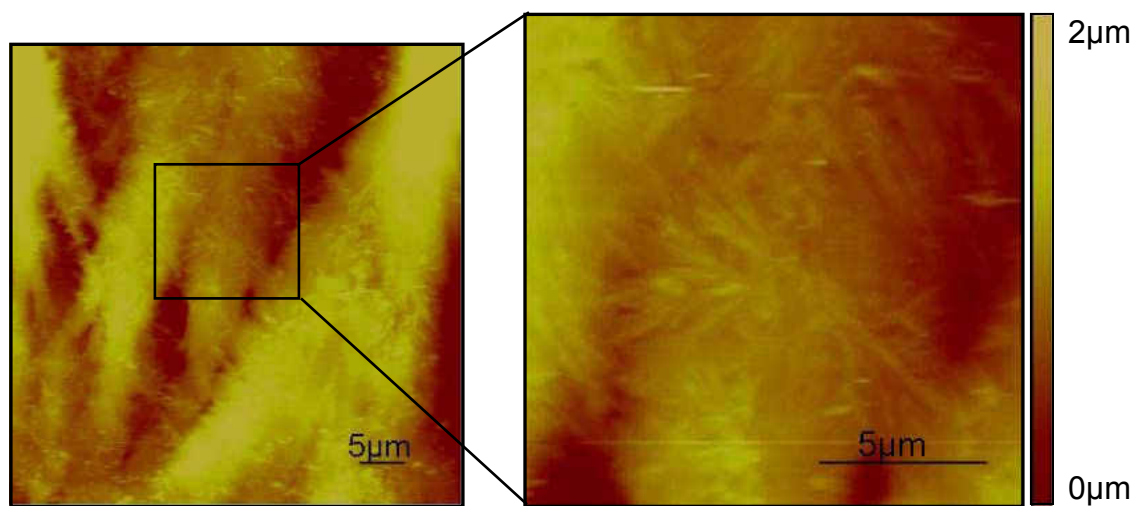


Figure 2.3 - Atomic Force Microscope image of packed fibers scanned after drying

The image on the left shows the long branched structures seen through the optical microscope previously. The gradient bar alongside the zoomed image shows the color profiling with respect to height in the images. The bright (yellow) regions have a greater height as compared to the dark (brown) regions.

Since it was difficult to obtain images of individual tubes on account of NaOH crystallization, the above sample was diluted to get better results. It was observed that after dilution the tubes/fibers formed short and straight aggregates that look like rigid, thick fibers [Fig. 2.4].

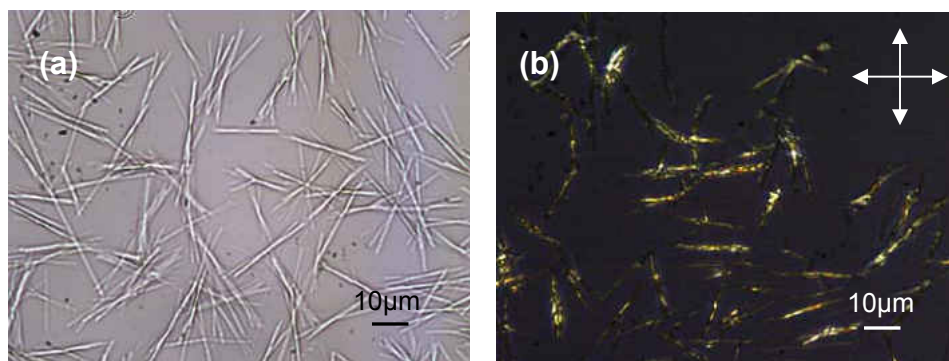


Figure 2.4 - Aggregates seen in the diluted sample (a) Bright field image (b) Image under cross polarizer

It was initially thought that these rod-like entities were individual tubes/fibers. However, AFM images confirmed that they were indeed collections of tubes/fibers. Some of these bundles are seen to aggregate further to form star-shaped structures as seen in Fig. 2.5. It is seen that there is an overlap of rods at the central portion of the star. There is an absence of symmetry in the star shaped structures which suggests that the rod-like aggregates are joined head-to-head and not at their centers. The cross section view [Fig 2.5(c)] of the star branches shows that the branches are spread out and flattened since their heights are about one order of magnitude smaller compared to their widths. This can be attributed to the fact that the self-assembled structures partially collapse and consequently, flatten during the drying process.

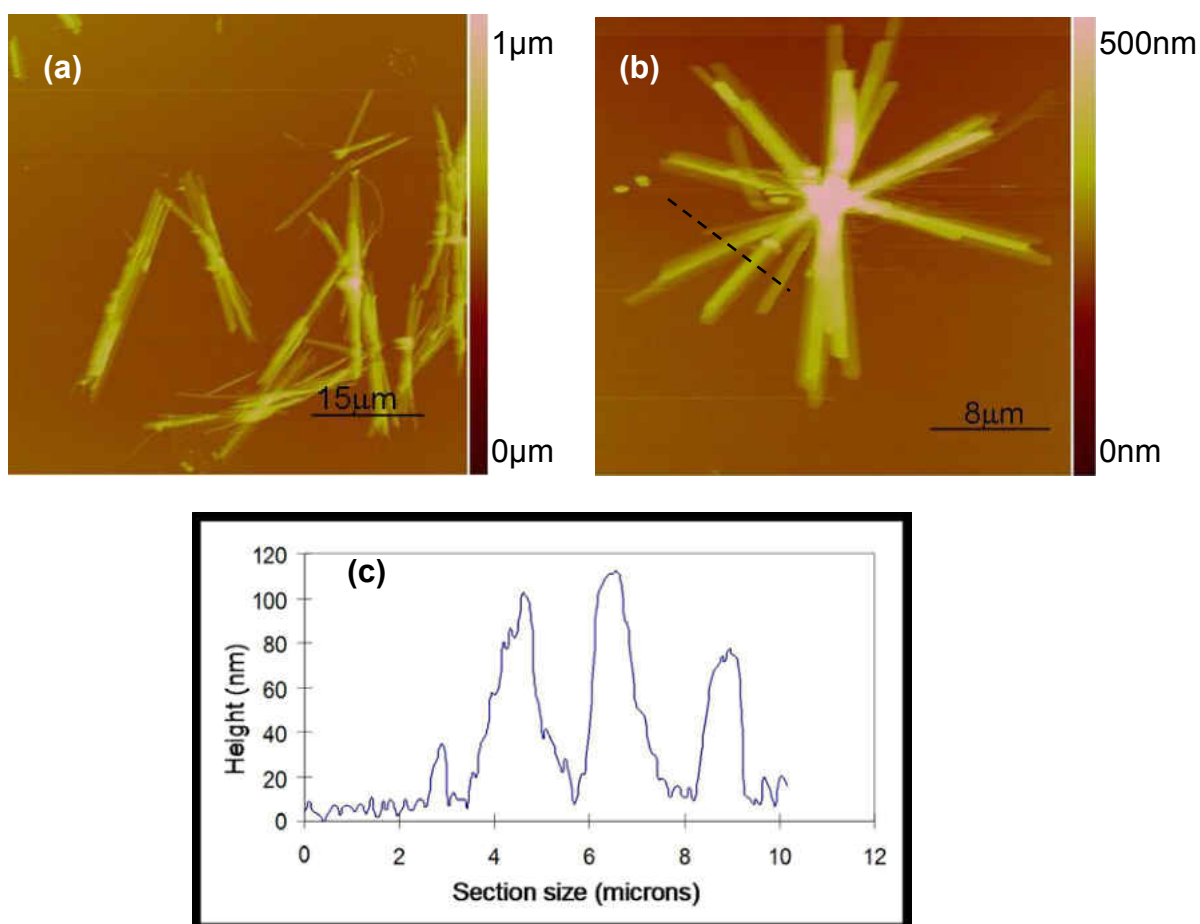


Figure 2.5 - AFM images of (a) Rod-shaped fiber aggregates (b) Star-shaped secondary aggregates (c) Cross-section view of star branches [taken at dotted line in (b)]

As the tubes and fibers grow, it gets harder for them to crystallize even on drying, which is why the long tubes that form at a later stage, adopt random coiled conformations and form “amorphous” type of aggregates [Fig. 2.6]. All the samples made at a high pH (about 12.5) contain these aggregates of coiled tubes/fibers. The size and number of the aggregates depends on a number of factors that will be discussed later.

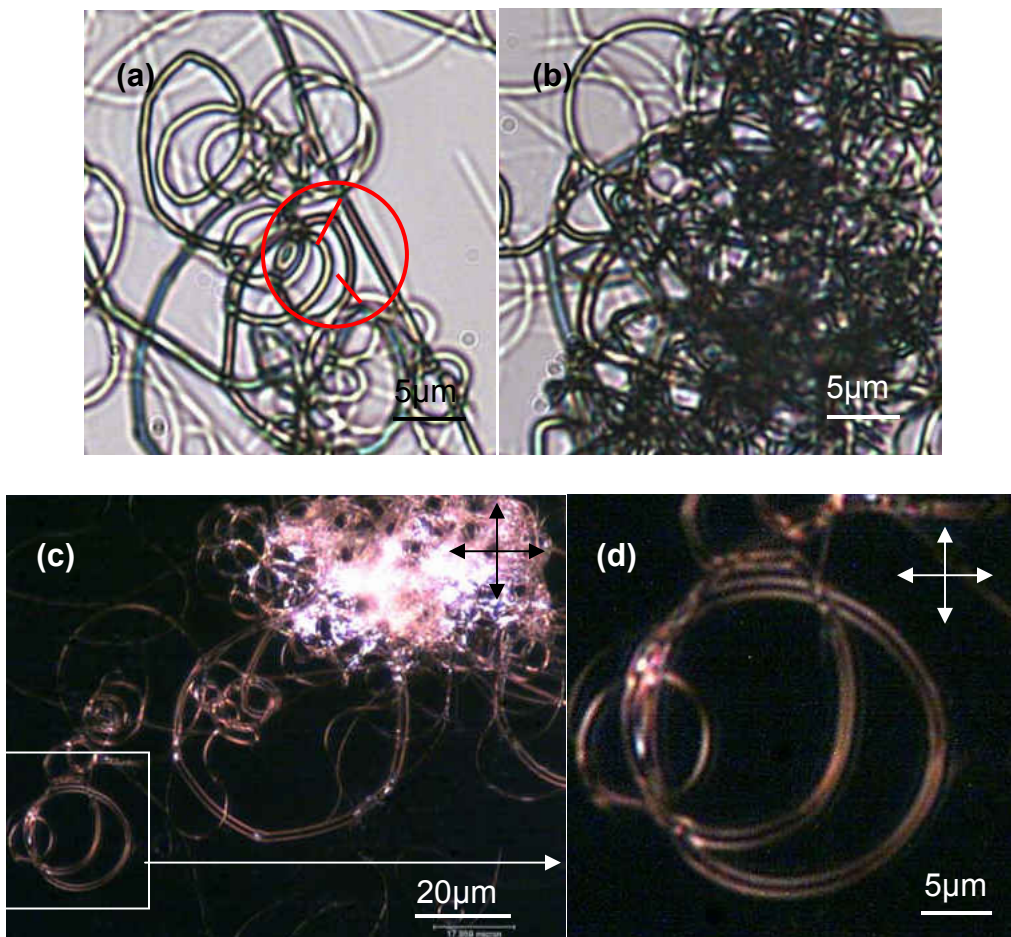


Figure 2.6 - Coiled tubes formed at high pH (a) segmental structure of tubes (b) aggregation of randomly coiled tubes (c) & (d) dark field images of the sample.

As mentioned previously, the long tubes are seen to form by the joining of shorter tubes. This can be seen from the segmental nature of the long tubes [shown in Fig. 2.6(a)]. It is seen that the length of the segments varies with the diameter of the tubes. This is expected as the rigidity of the tubes increases with the increase in diameter (and, as a result, in the wall thickness). Hence the persistence length of the tubes is variable depending upon the diameter and the wall thickness, thus leading to different amounts of flexibility and curvature in the tubes. Fig. 2.6 (b) shows the aggregation of the

randomly coiled tubes to form disordered clusters while Fig. 2.6 (c) shows a cluster as well as free tubes under cross polarizers. The hollowness of the structures confirms that they are indeed tubes [Fig. 2.7]. The thickness of the tube in the figure is about 800nm while its internal diameter is about 1 μ m. It was noted that the value of the wall thickness was comparable to the inner diameter of the tube. For thinner tubes, thus, the internal hollow becomes almost negligible in size and we can call them as fibers. The tubes are not monodisperse and they vary in length as well as diameter. Also, the tube walls display birefringence under cross polarizers which is a common characteristic observed in the LCA samples we studied. This suggests that LCA, a chiral molecule in itself, also forms chiral supramolecular assemblies.

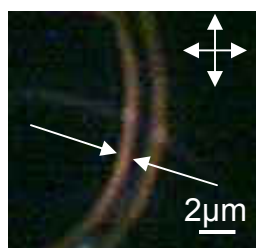


Figure 2.7 - Hollow structure of the self-assembled structures

In order to study the aggregation behavior of the coiled tubes, reaction conditions were varied systematically and their effect on the sample was noted. A detailed description of these experiments now follows.

Change in LCA concentration

The concentration of LCA was changed from 0.075% w/w to 4% w/w to observe its effect on the sample. Fig. 2.8 shows optical microscope images of samples with LCA concentration from 0.075% to 0.25%. All the samples are seen to contain white aggregates of coiled or coiled tubes or fibers packed in a random fashion.

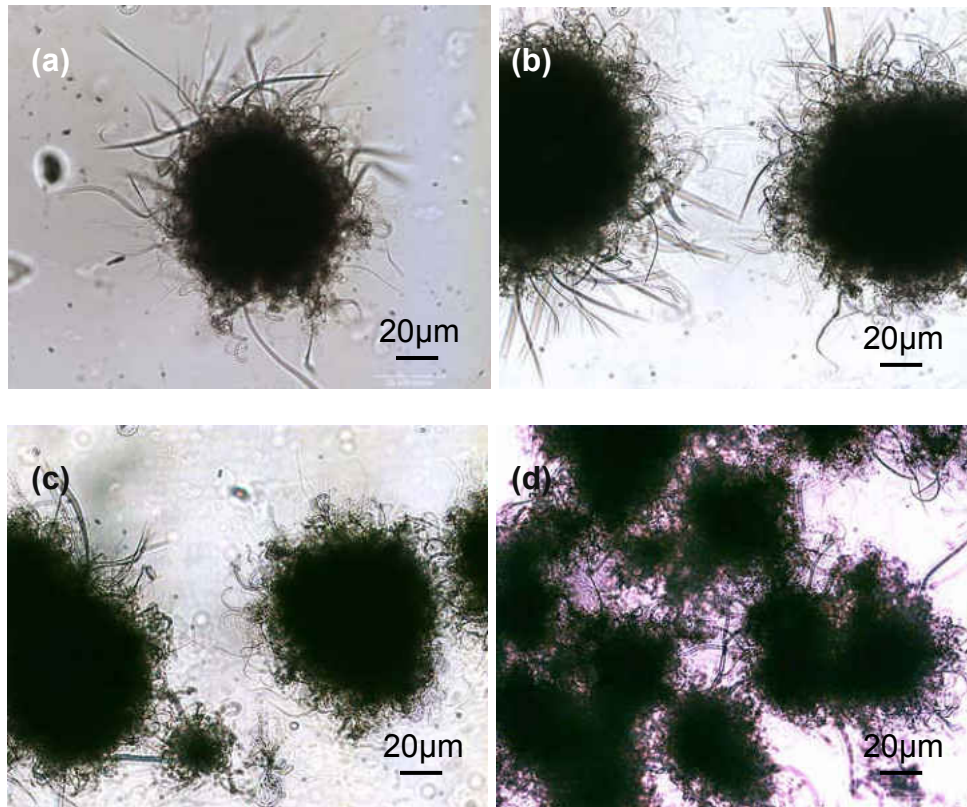


Figure 2.8 - LCA concentration change in the lower range. (a) 0.075% (b) 0.15% (c) 0.2% (d) 0.25%

It is seen that as the concentration increases, the number of the aggregates increases from low concentration to higher concentration. The reason for this could be the increase in the number of nucleation sites for aggregate formation. It is hard to comment on the effect of LCA concentration on the size of the aggregates as the

samples are polydisperse with respect to aggregate size. However, a rough trend suggests that the aggregate size increases till 0.15% LCA and decreases on further increase in concentration as shown in Fig. 2.9. This can be explained by the fact that the number of aggregates increases rapidly with concentration. Thus, a large increase in numbers accompanying a small increase in concentration should result in reduction of aggregate size.

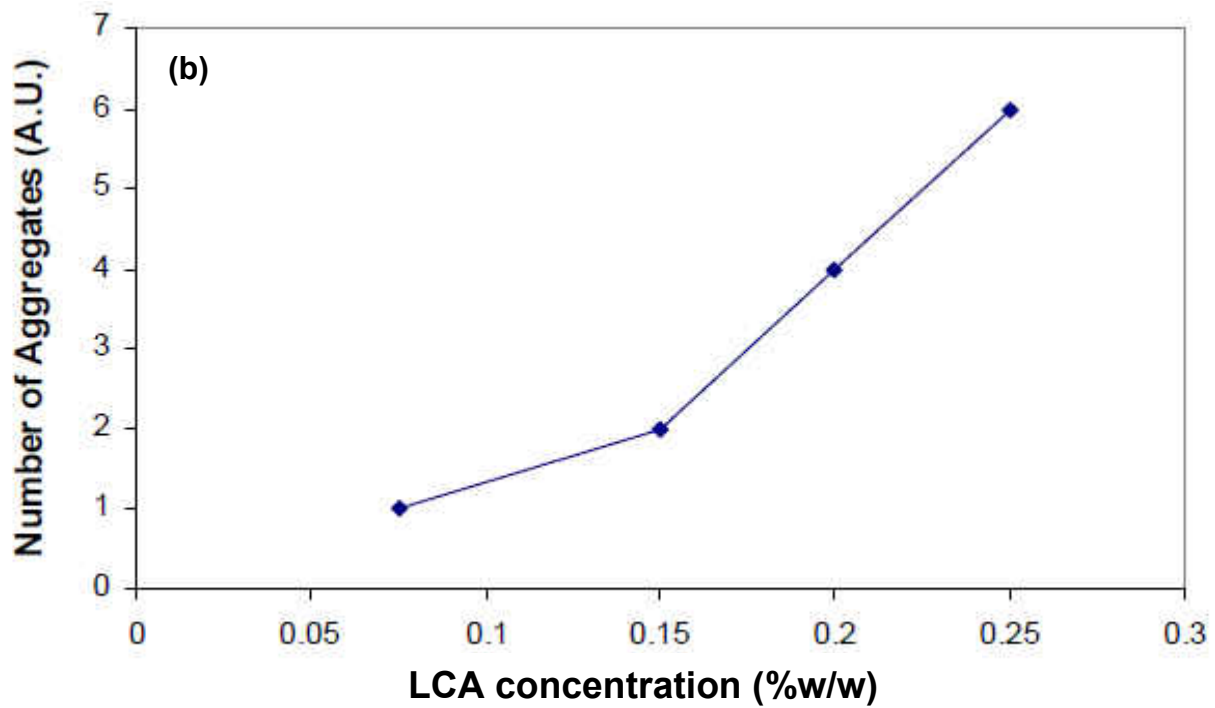
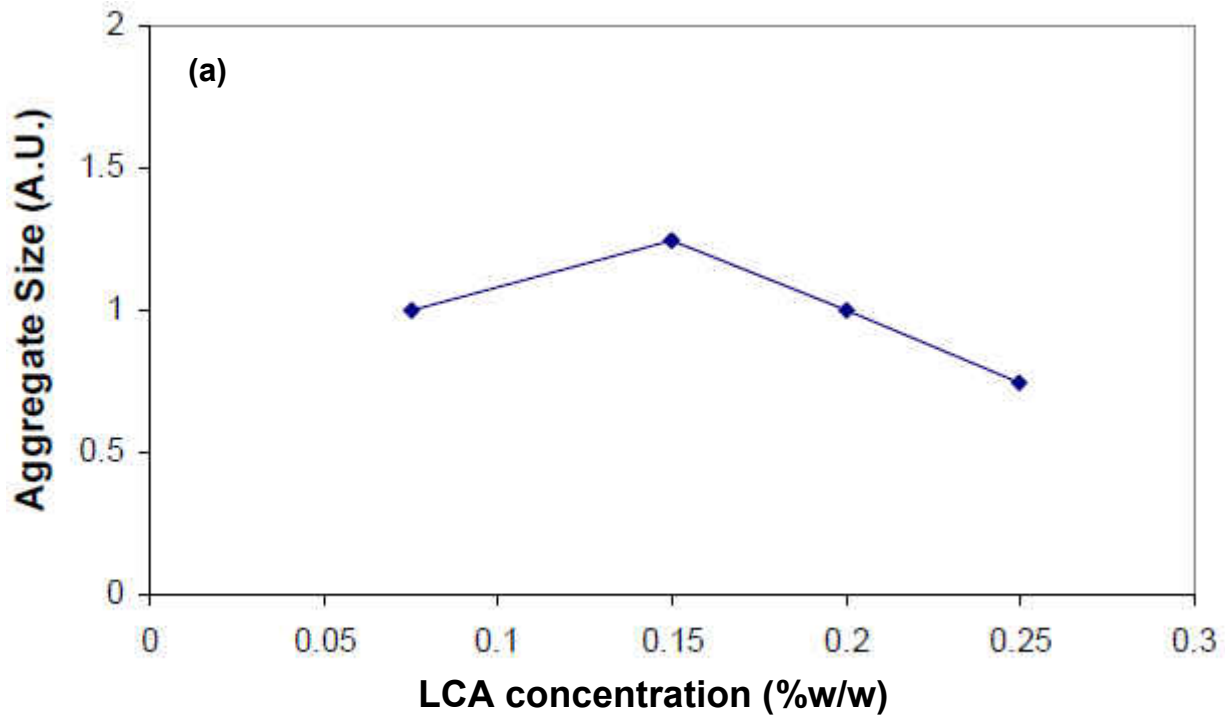


Figure 2.9 - Change in morphology with respect to LCA concentration (a) Effect on aggregate size
(b) Effect on aggregate number

For the high concentration range (1-4%w/w) the samples show a different kind of behavior. These samples exhibit advanced aggregation very late as compared to the low concentration samples. It is proposed that when the concentration increases beyond a certain level, very thin fibers form in the sample. The thin tubes are thought to form a network in the solution, thus increasing its viscosity. Due to high viscosity of the samples, it is hard for the molecules to migrate and aggregate easily. Thus, the smaller tubes form arrangements that are barely perceptible under the optical microscope as compared to the aggregates observed in low concentration solutions. These samples display birefringence under cross polarizers [Fig. 2.10 (b)]. The solution looks translucent white due to the small size of the aggregates. The sample does not turn white soon since it takes more time to form big enough aggregates that scatter light.

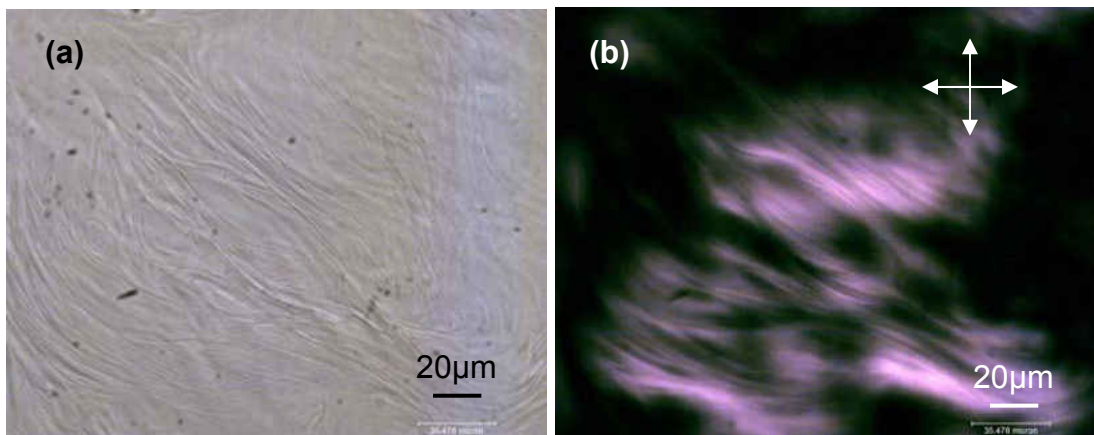


Figure 2.10 - Samples with high concentration of LCA (a) bright field image (b) dark field image

Change in NaOH concentration

The molar concentration of sodium hydroxide was varied from 0.05M to 0.8M in order to study its effects on the self-assembly of LCA. It was seen that the rate of formation of tubes and fibers increased with increase in NaOH concentration for low concentrations. As the concentration increases to higher values, it is seen that the formation of tubes/fibers becomes less favorable. Fig. 2.11 shows the variation of morphology of the fibers with respect to NaOH concentration for lower values of solution strength. The aggregates formed in lower sodium ion concentration have longer and more pronounced branches.

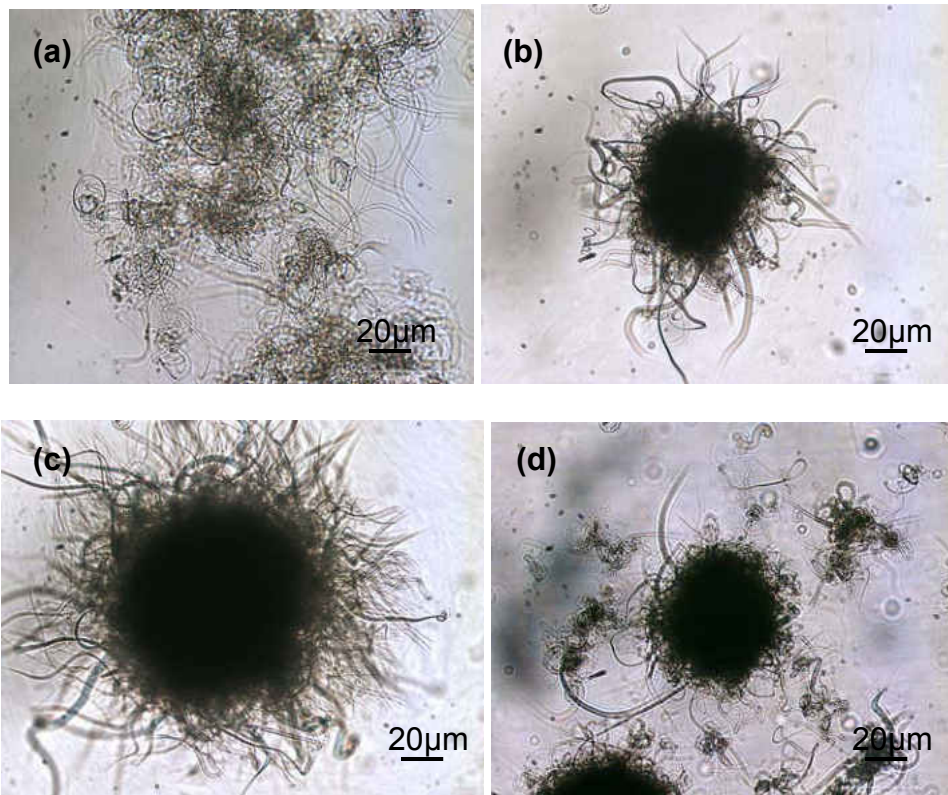


Figure 2.11 - Effect of NaOH concentration on morphology (a) 0.05M (b) 0.075M (c) 0.1M (d) 0.15M

It is seen that when the strength of the NaOH solution is very high, tubes/fibers do not form in it. It also appears that the mechanism of formation of the aggregated tubes/fibers is different in high strength NaOH solutions [Fig. 2.12]. At extremely high NaOH concentrations (near 0.8M) the solution contains only LCA platelets. As the strength decreases, fibrous growth is seen to sprout from the edges of the platelets. The length of these outgrowths increases with decrease in NaOH concentration. The LCA concentration was kept constant at 0.1% in all samples.

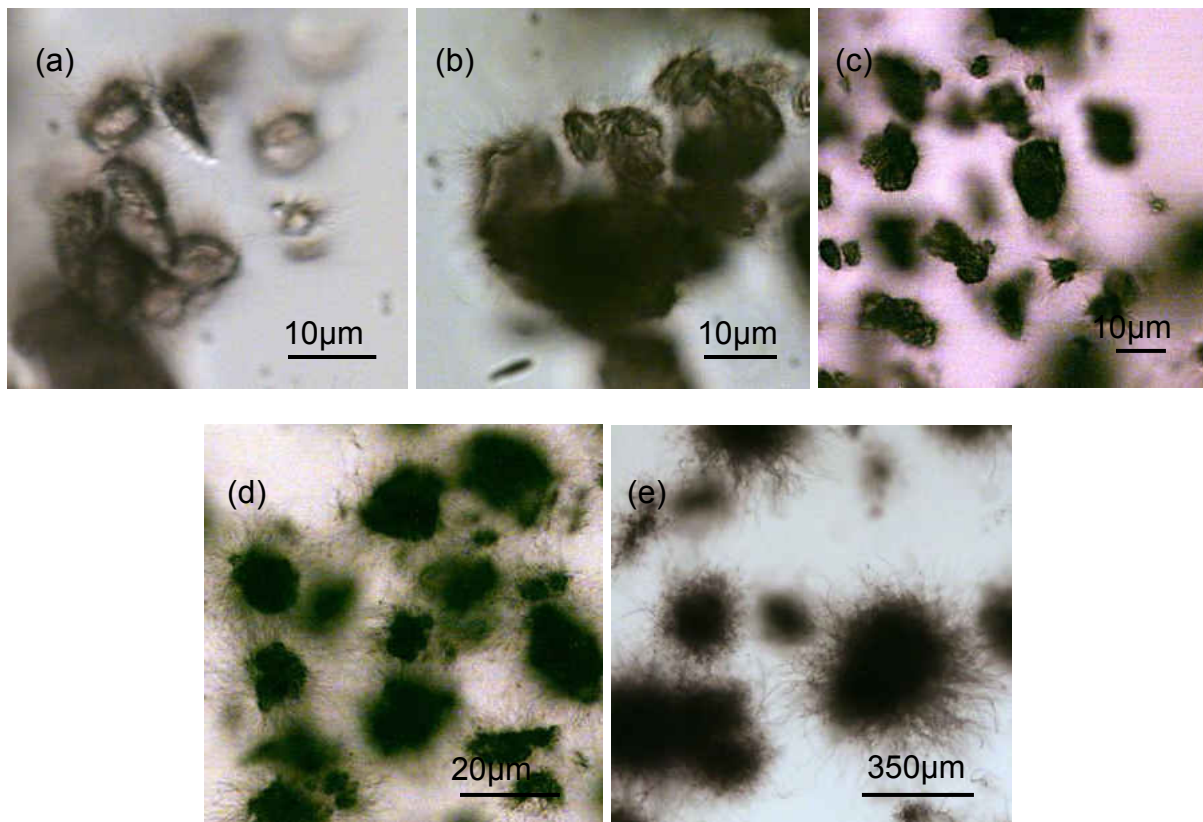


Figure 2.12 - Change in morphology of aggregates with different NaOH solution strength (a) 0.8M (b) 0.5M (c) 0.4M (d) 0.3M (e) 0.2M

Effect of sonication

Aggregated samples like the ones shown above, when subjected to intense sonication for about 30 minutes, were seen to break apart into individual tubes/fibers. The aggregates were not entirely broken down into individual fibers. However, they visibly reduced in size and the surrounding solution was seen to fill up with the broken shorter tubes [Fig. 2.13]. Due to intense sonication, the solution gets warmed up slightly but the final temperature is well within the thermal stability range of the fibers. It can be clearly seen that the tubes and fibers stay coiled and flexible after sonication. They are visibly shorter than the long entangled fibers in the aggregates.

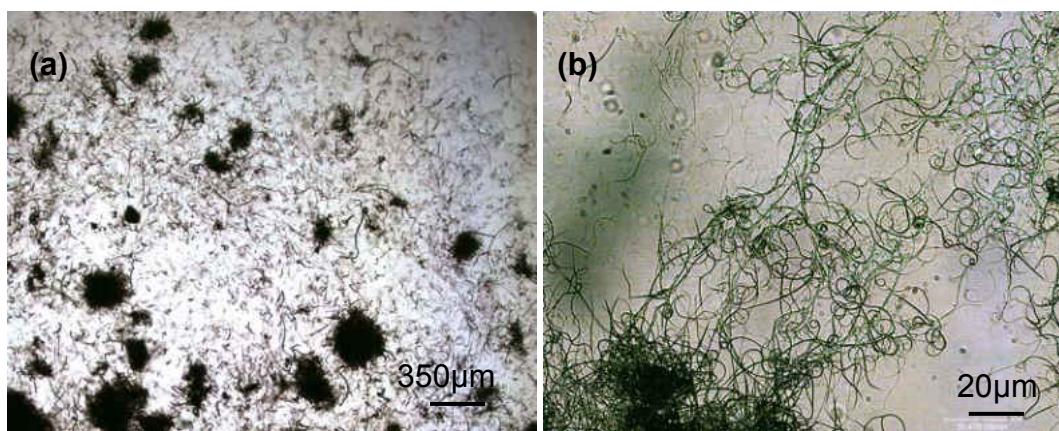


Figure 2.13 - Sample with 0.25% LCA and 0.1M NaOH broken down on sonication

It is observed that on addition of water to the sample, the tubes tend to straighten up [Fig. 2.14]. This is attributed to the fact that the pH of the solution reduces as water is added to it. In further discussions it will be explained⁵ how samples behave at lower pH values and the reasons behind such behavior.

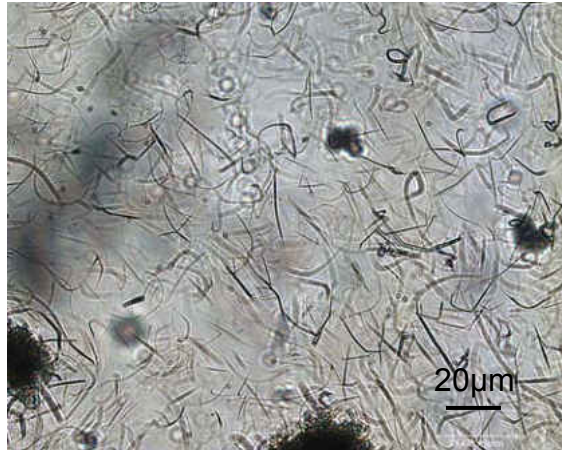


Figure 2.14 - Sonication after addition of water

Effect of Temperature

It was noted that when high concentration samples were heated to moderately high temperatures (about 65 to 68°C) in bulk form, they formed solid, white gels^[62] that retained all the water from the solution. A special sample with an intermediate LCA concentration (0.5% w/w LCA) was prepared to test for gel formation. The sample was placed in a glass vial and heated in a copper element heater for about 30 minutes at 66°C. The sample did not show significant aggregation before heating. Once the thermal processing was conducted, a thick network of tubes and fibers was seen all over the sample. This phenomenon enlightened us to the importance of temperature in affecting molecular mobility and, consequently, molecular arrangement. The density of the gel was found to increase with increase in initial LCA concentration in the sample. However, these solid gels formed only when the sample was heated in bulk for an extended period of time (at least 30 minutes). Also, it was necessary for the sample to have achieved a certain extent of self-assembly (a particular number of tubes/fibers present) in order to gelate.

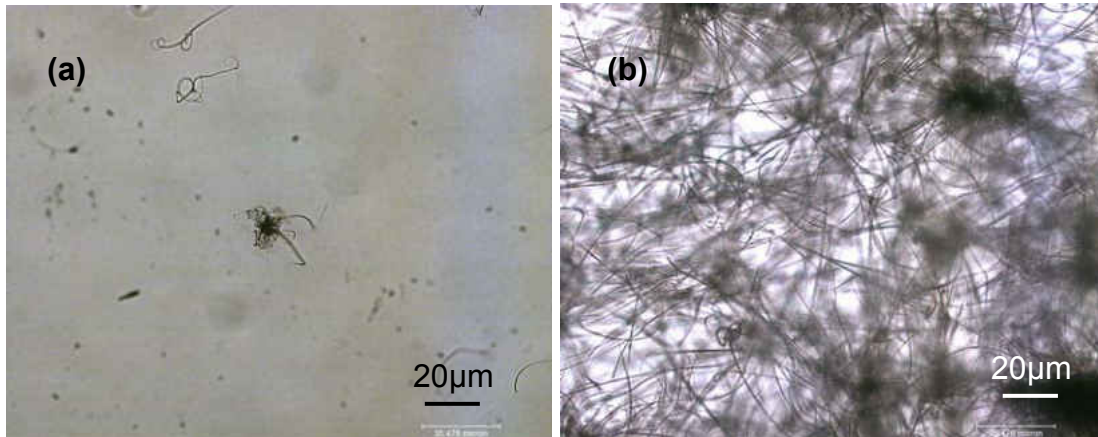


Figure 2.15 - Formation of dense gels through thermal processing (a) Before heating (b) After heating

2.3 Synthesis and Properties of Straight Sodium Lithocholate Tubes and Fibers

2.3.1 Experimental Method

Straight tubes were synthesized using a modified procedure based on the one described in section 2.2.1. In this experiment, 0.1% w/w LCA was added to 0.1M NaOH solution and mixed on the vibrator for a minute. The solution was then allowed to stand for a couple of hours at room temperature. The pH of this solution was noted to be between 12 and 13. After letting the sample stand, water was added in it to lower the pH to a value of about 7. The sample was then allowed to stand for the self-assembly process to continue.

2.3.2 Results and Discussion

2.3.2.1 Formation of Tubes and Fibers

As explained earlier, when LCA is dissolved in basic solutions in concentrations above 0.05% w/w it can self assemble into macromolecular structures. The self-assembly starts out by the formation of spherical micelles or vesicles, which later on fuse to form cylindrical or rod-like structures. As seen previously, in the range of concentration near 0.1% LCA and a solution strength of 0.1M NaOH, the rate of self-assembly increases with increase in concentration as well as with the NaOH strength. Thus, when the pH of the sample is lowered, the rate of self-assembly is expected to reduce too. In this experiment, in order to avoid the possibility of diluting the solution below the critical micelle concentration, the vesicles were allowed to form in high pH before the pH was lowered by dilution.

2.3.2.2 Morphology of Tubes and Fibers

About 3 weeks after synthesis, the sample was seen to turn milky white and was observed under an optical microscope. The structures observed were straight and rod-like [Fig. 2.16 (a)]. Aggregation was present in this sample as expected^[41]. The nature of the aggregates, however, was different in that most of them existed as rigid rod-like collections of tubes which further organized into star-shaped (spherulite – like) aggregates with the rods protruding radially outward from a central point [Fig. 2.16 (b)]. This behavior was also previously noted in case of the high pH sample diluted to form

short straight tubes (section 2.2.2.2). The rod-like clusters were rigid and were seen to branch out at one or both ends.

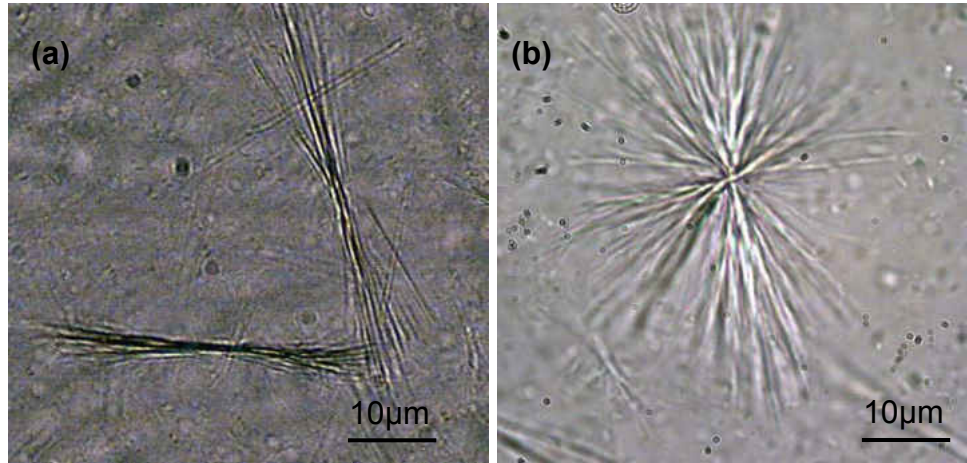


Figure 2.16 -Aggregation in samples made at low pH values

In case of the straight tubes, the aggregates undergo a lot of changes which can be studied using an optical microscope. The aggregates are seen to increase in size and number with time. It is a known fact that rigidity depends on length and wall thickness so as the fibers grow longer, they start getting thinner and more flexible [Fig. 2.17].

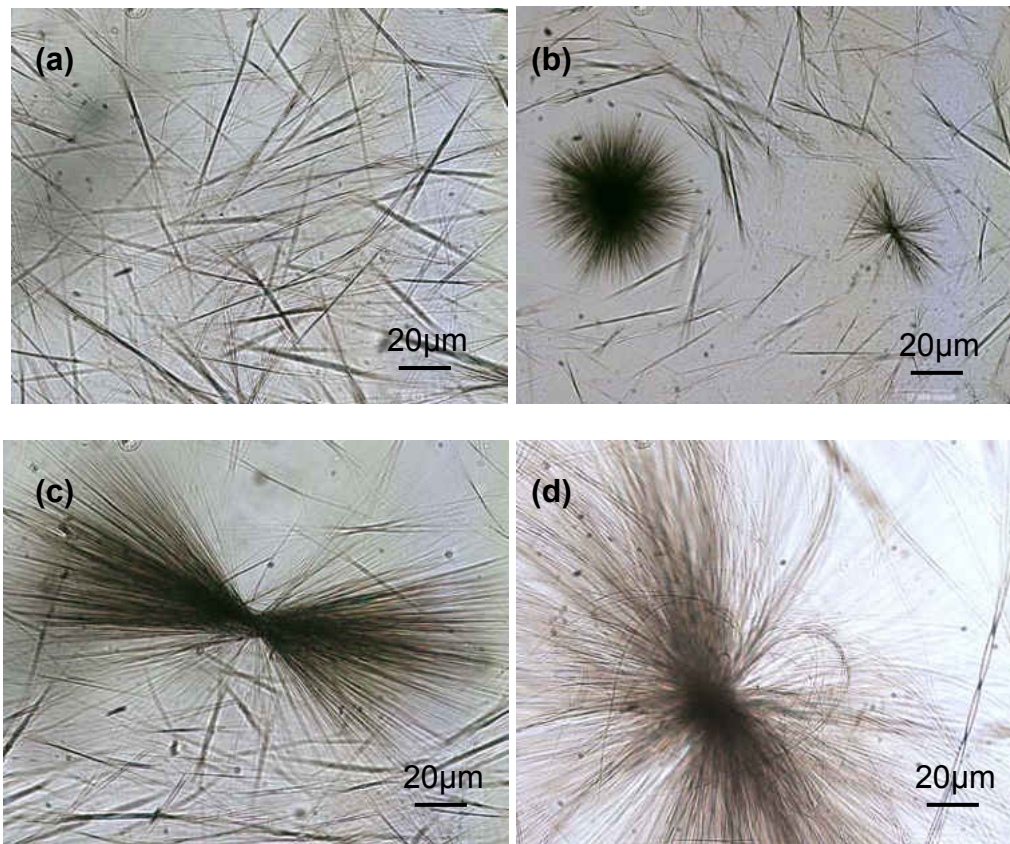


Figure 2.17 - Progression of growth of self-assembled aggregated structures at pH 7 (a) rod-like initial aggregates (b) star-like secondary aggregates (c) star-shaped aggregates grow and branches become thin (d) branches grow long enough to become flexible and bend.

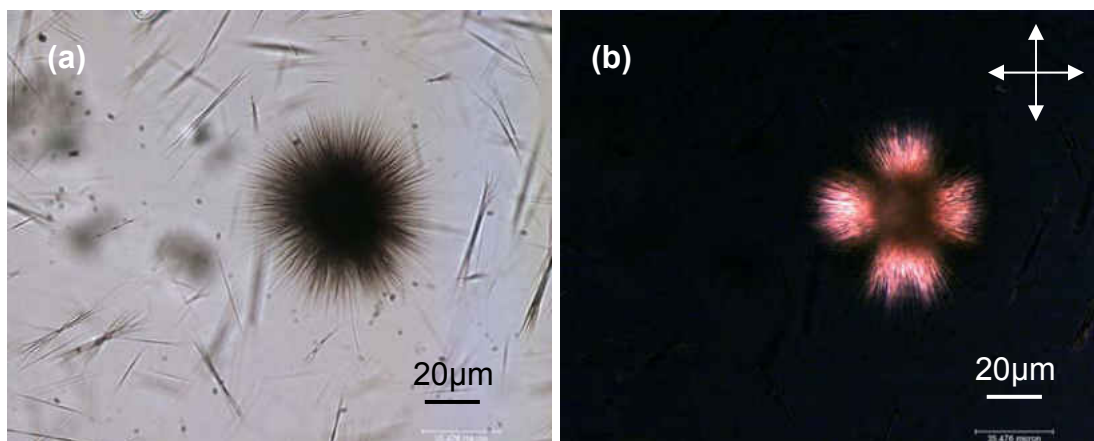


Figure 2.18 -Birefringent patterns shown by aggregates (a) Optical image and (b) Corresponding dark field image

As shown above, when the sample is observed under a cross polarizer, it shows birefringent patterns as in case of the coiled tubes. The fibers light up in the directions where the molecules are packed at an angle to both, the polarizer and the analyzer. In places where the molecules are parallel to either one of the polarizers, the intensity of transmitted light is zero.

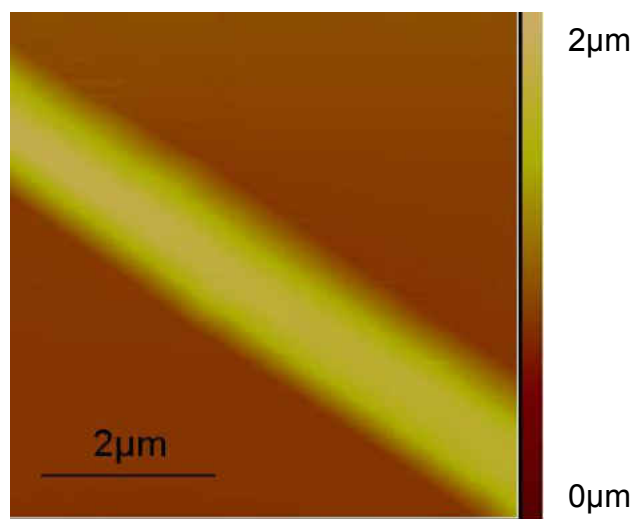


Figure 2.19 - AFM image of a straight fiber

The average size of the straight tube is seen to be around $1.3\mu\text{m}$ from the AFM image shown in Fig. 2.19. It appears that the surface of the tube/fiber is very smooth and uniform.

Similar to the samples prepared at high pH, the straight tubes/fibers were sonicated as well. After 30 minutes of sonication, they broke up from the aggregates in a similar fashion [Fig 2.20] and they remained straight after they broke apart. The lengths of the sonicated fibers were seen to lie within a narrow range of values and the distribution is shown in Fig. 2.21.

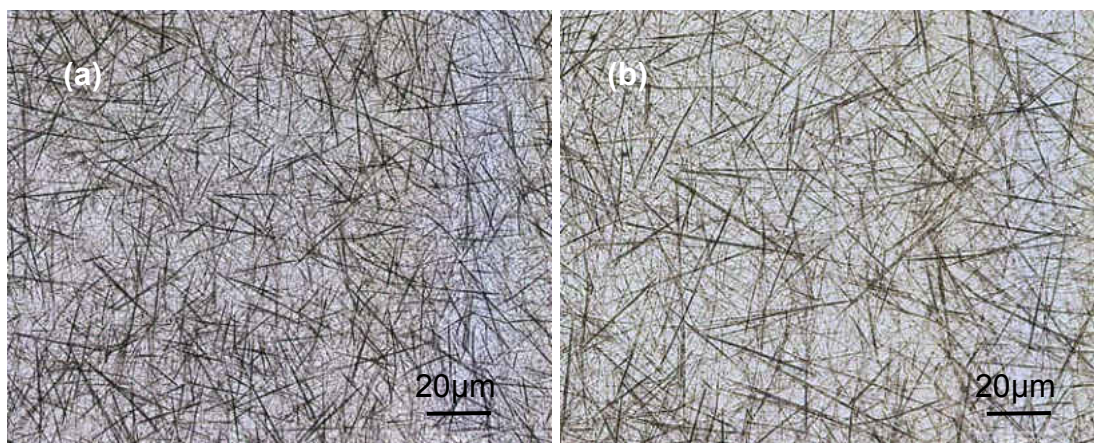


Figure 2.20 -Broken down fibers after sonication

This experiment suggests that the tubes/fibers can be shortened simply by using mechanical means. This makes sense because of the fact that all the molecules in the fibers are held together by weak secondary forces.

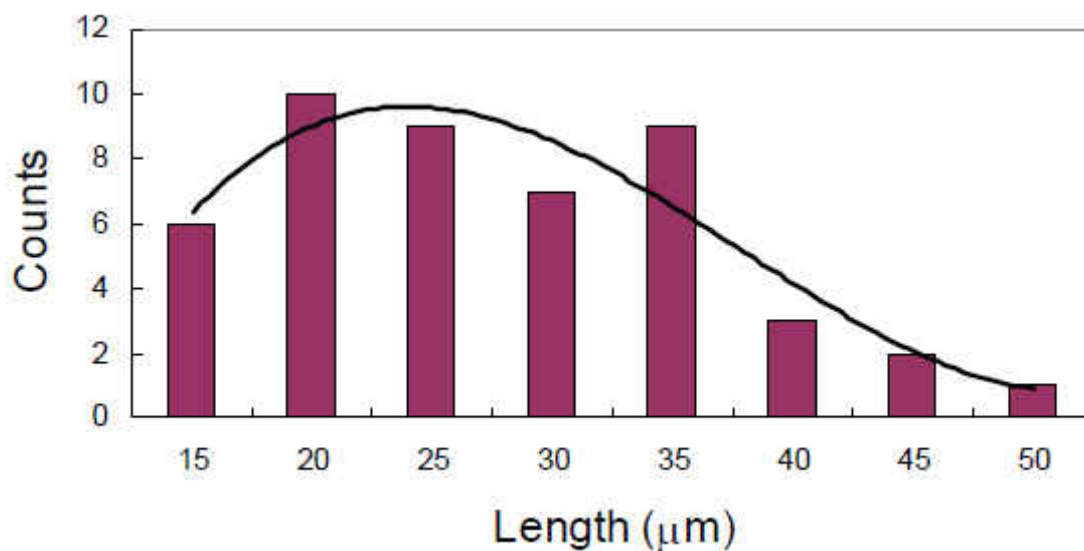


Figure 2.21 - Length distribution of sonicated straight fibers

The average length of the sonicated tubes/fibers is about 25μm and is seen to vary mostly from 15 - 35μm. Thus, sonication is a method by which de-aggregation can be achieved. Moreover, the length of the tubes can also be manipulated to suit our requirements.

Effect of salt

It is a well-known fact that salts alter the hydrophobic interactions present in aqueous solutions of non-polar solutes. This occurs due to the changes in entropy of the hydrogen-bonded water network and/or enthalpy effects of surface creation.^[63] It has been observed that generally sodium chloride in appropriate quantities leads to increase in the hydrophobic interactions of non-polar solutes in aqueous solutions.^[64-65] Kokkoli and Zukoski used a novel approach and demonstrated this using an Atomic Force Microscope.^[66]

Measured quantities of common salt (NaCl) were introduced in equal volumes of the dispersion containing straight tubes/fibers. All samples were drawn from the same parent solution [Fig2.22 (a)]. It was seen that the introduction of salt led to the increase in the size of the star-shaped aggregates and rendered their branches flexible [Fig 2.22(b-d)]. It is speculated that since NaCl induces strengthening of hydrophobic interactions, the star-shaped aggregates increase in size on addition of LCA molecules on them. The increase in branch length and the incorporation of salt in the solution (which brings about charge screening) are thought to cause the branches to curve and partially fold on themselves.

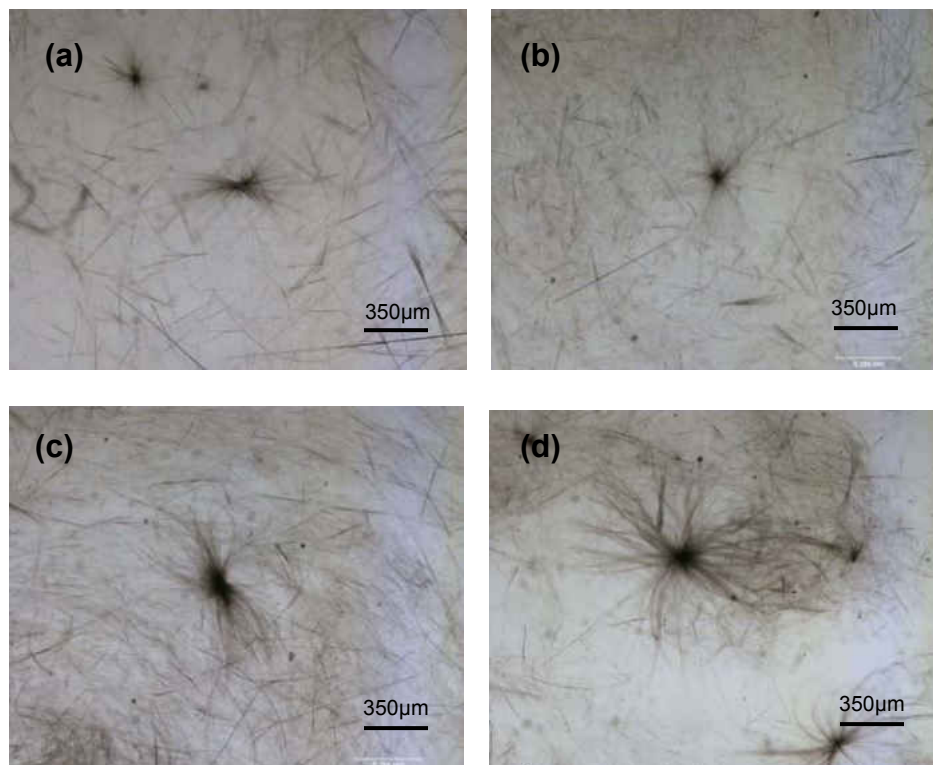


Figure 2.22 - Effect of sodium chloride on the morphology of straight rods and tubes (a) original sample (b) 7.5mg/ml NaCl (c) 25mg/ml NaCl (d) 100mg/ml NaCl

2.3.3 Mechanical Properties of Different Tubes

The AFM can be used to estimate the mechanical properties of soft materials through various methods. The method employed in this study was the cutting method [Fig. 2.22]. In this method, the tubes were subjected to repetitive scanning at a single point under similar conditions in order to compare the stiffness of both the straight and the coiled tubes. One representative fiber was picked from each sample for the experiment. Both these fibers had similar diameters so as to ensure uniformity of the experiment. The scan was carried out in the direction perpendicular to the length of the fibers. The force used for scanning was about 290nN and the fibers were subjected to 40 scans each. It was seen that the coiled tube was cut in half but the straight tube endured the scanning. This proves that the straight tubes are indeed more rigid compared to the coiled ones as expected.

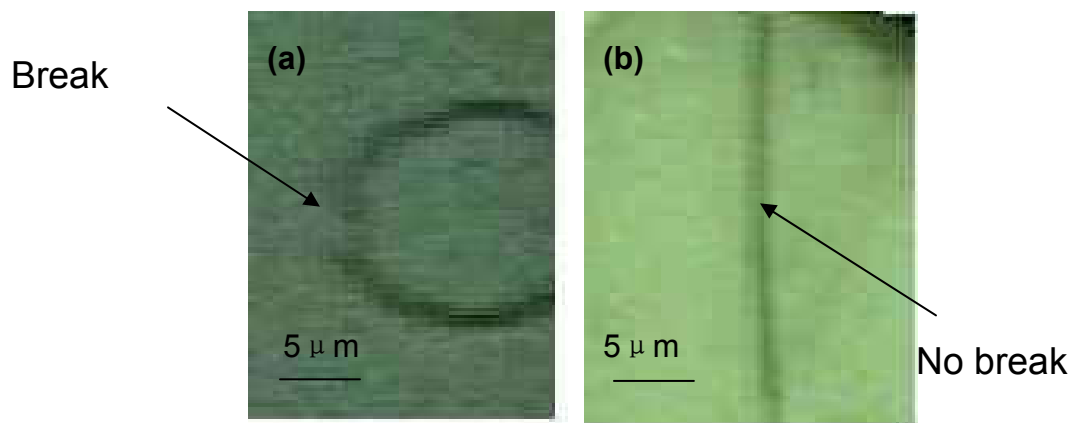


Figure 2.23 – Assessment of mechanical properties using the cutting method (a) Curved tube and (b) Straight tube

FTIR results [Fig. 2.23] show peaks at 1440 cm^{-1} and 1546 cm^{-1} for both the coiled and the straight tube samples which represent the formation of a lithocholate ion due to deprotonation. In case of the straight tubes, however, there also exists a peak at 1736

cm^{-1} denoting the presence of the acidic group in the molecule ^[67]. Thus, we can say that the LCA is only partially deprotonated in case of the straight tubes. Hence, there is a greater chance for the LCA molecules in the straight tubes to form hydrogen bonds with their neighbors. Since there is a greater amount of hydrogen bonding, the straight tubes are stronger and more rigid.

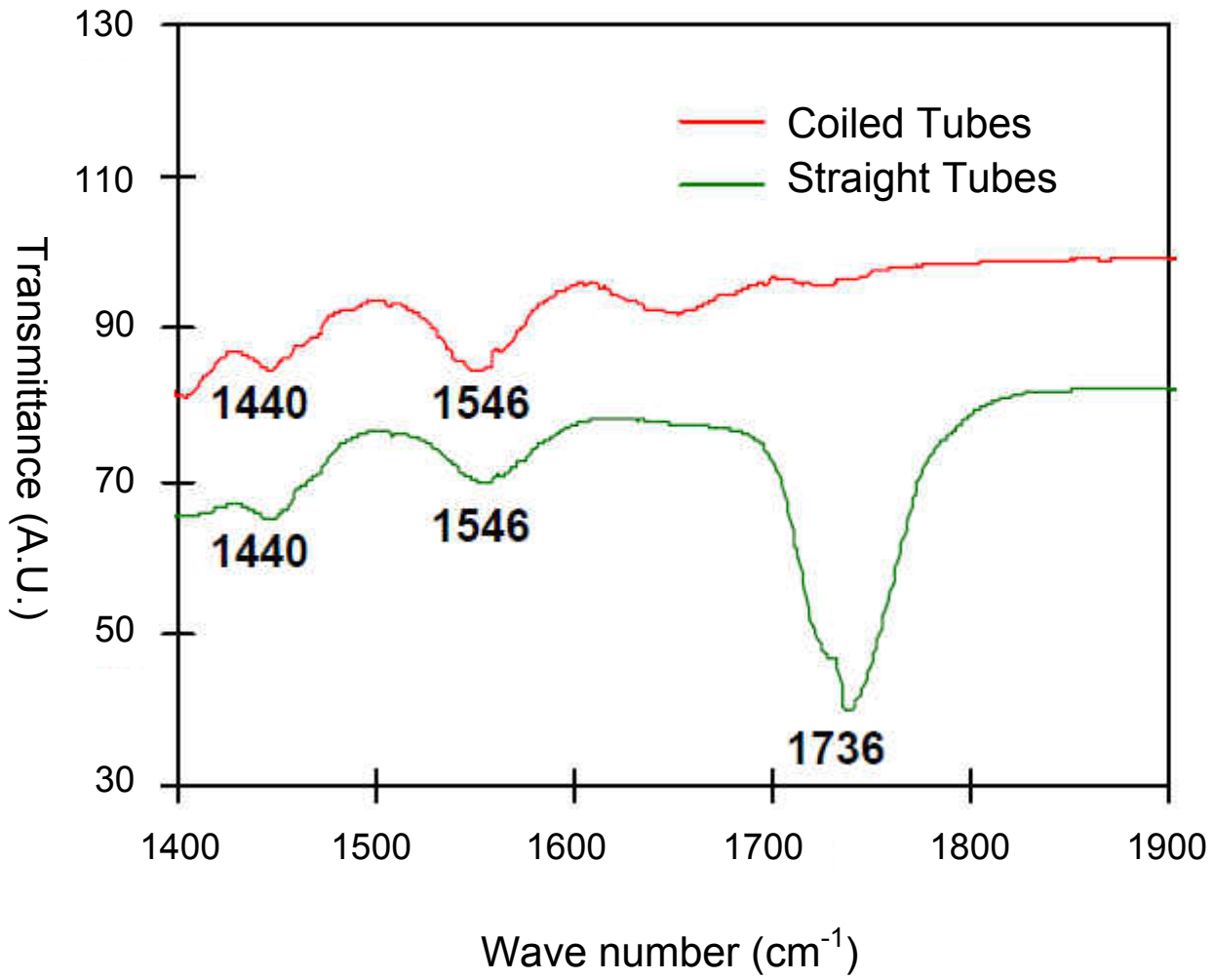


Figure 2.24 - FTIR scans of coiled and straight tubes

2.4 Synthesis and Properties of LCA Fibers Using Organic Bases

The sodium lithocholate system was studied extensively with respect to its morphology, growth and aggregation characteristics and responsiveness to external conditions. In order to investigate the effect of the nature and size of the counterion on the process of self-assembly, organic bases like ethylamine (EA) and ethylene diamine (EDA) were employed in place of sodium hydroxide. The synthetic procedure was identical in both cases and is described in section 2.4.2. The structures of EA and EDA are discussed in the following section in order to present a clearer picture of the kind of change the system would undergo due to NaOH replacement.

2.4.1 Structure of Organic Bases Employed

2.4.1.1 Ethylamine

Ethylamine is a primary amine which is the second member of the homologous series of aliphatic straight-chain primary amines. It has a structure as shown in Fig. 2.24 and is a weak base that can nevertheless provide an environment that is conducive for the LCA molecules to self-organize. Ethylamine exists naturally as a gas and was thus used in the form of its aqueous solution (70% w/w).

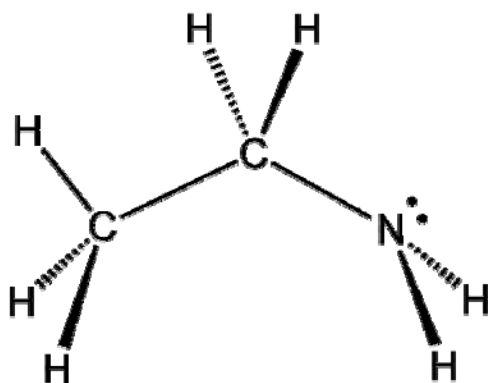


Figure 2.25 - Ethylamine

2.4.1.2 Ethylenediamine

Ethylenediamine is a bifunctional molecule with two terminal -NH_2 groups acting as the electron-donating groups. It is a strong base capable of deprotonating LCA. Since it has two amino groups, it is more effective in deprotonation of the acid compared to ethylamine. An aqueous solution of 30% ethylenediamine was used to prepare the mother solution for fiber synthesis.

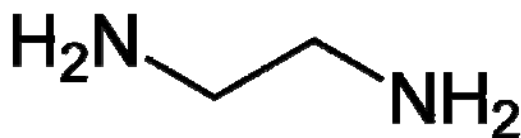


Figure 2.26 – Ethylenediamine

2.4.2 Experimental Method

Both the organic bases in consideration are highly water soluble on account of being capable of extensive hydrogen bonding in water. They were dissolved in water so as to form 0.1M solutions in both the cases. The appropriate amount of LCA was then added

to the solutions to make samples containing 0.1% w/w LCA. The samples were made at room temperature.

2.4.3 Results and Discussion

2.4.3.1 Formation of Fibers and Tubes

The organic bases deprotonate the carboxylic group of LCA and help dissolve it in the solution. The degree of deprotonation is different in different samples. It depends on various things such as the strength of the base, the size and conformation of the basic molecule and the interactions between the various molecules present in the solution. On dissolution of LCA, the molecules self-assemble into fibers and tubes as in case of sodium lithocholate samples. The size and morphology of the tubes, however, is quite different in both the cases.

2.4.3.2 Morphology of Fibers and Tubes

EDA sample

In case of both the EDA and the EA samples, a large number of structures were seen to form quite early in the self-assembly process. On day 5 after synthesis was carried out, the EDA sample showed aggregate formation similar to ones seen in straight sodium lithocholate (SLC) samples. The main difference that was observed between the EDA sample and straight SLC sample was that the EDA sample aggregates did not have straight branches. Neither did they aggregate in a totally random fashion as in case of the coiled SLC samples. The exact details can be visualized in the optical images shown in Fig. 2.26.

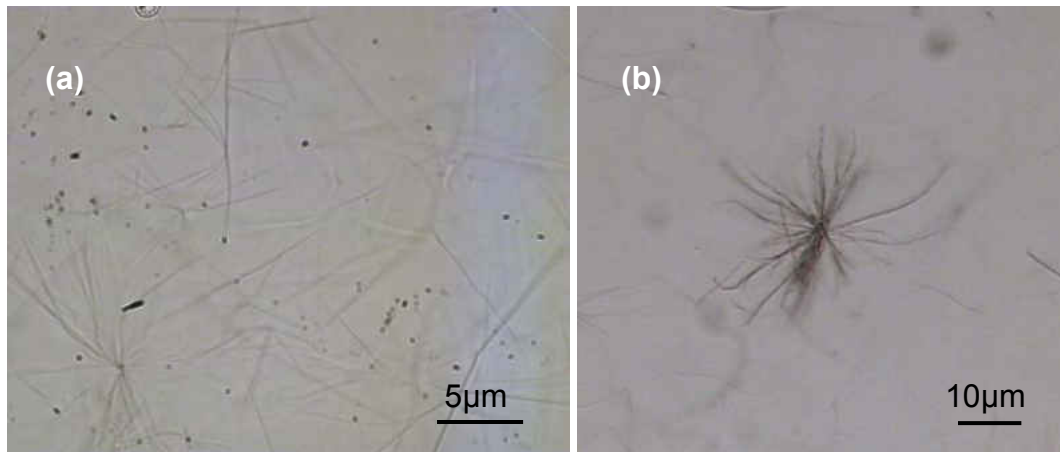


Figure 2.27 - EDA sample (a) Individual fibers/tubes on day 2 (b) Aggregation on day 5

The fibers and/or tubes are seen to grow with time as expected. The mechanism of growth is not clear yet but based on AFM images, it is speculated that it takes place layer by layer. The image in Fig. 2.28 (b) shows fibers present in the EDA sample and the circle marks the area of growth. It can be seen that the lower half of the marked fiber is thicker in diameter compared to its top half. It is thought that the fibers grow by the deposition of material layer by layer or by wrapping up of plates over existing fibers/tubes.

The growth of EDA sample was proved by studying the sample 6 months after synthesis. The images are shown in Fig. 2.27.

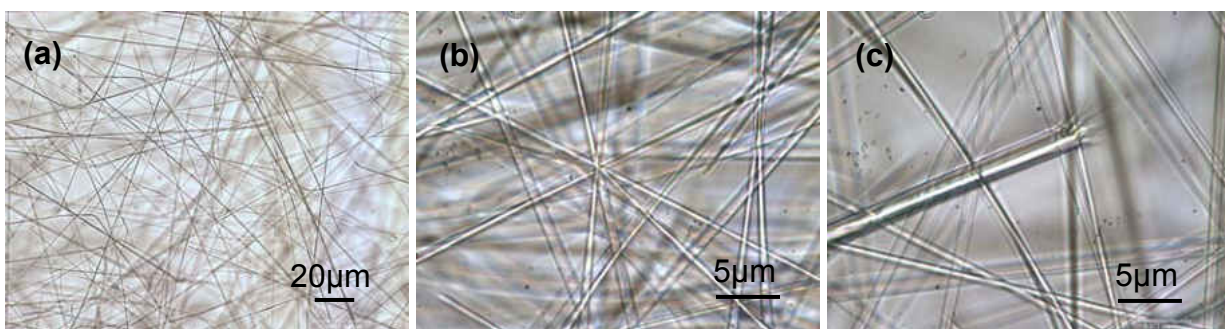


Figure 2.28 - EDA sample 6 months post synthesis

The growth of the tubes/fibers is clearly seen in the above images. Most of the structures are very long (more than 200 μm long) and some of them are as thick as 3 μm in diameter [Fig.3.27(c)] which is seen in the AFM images as well

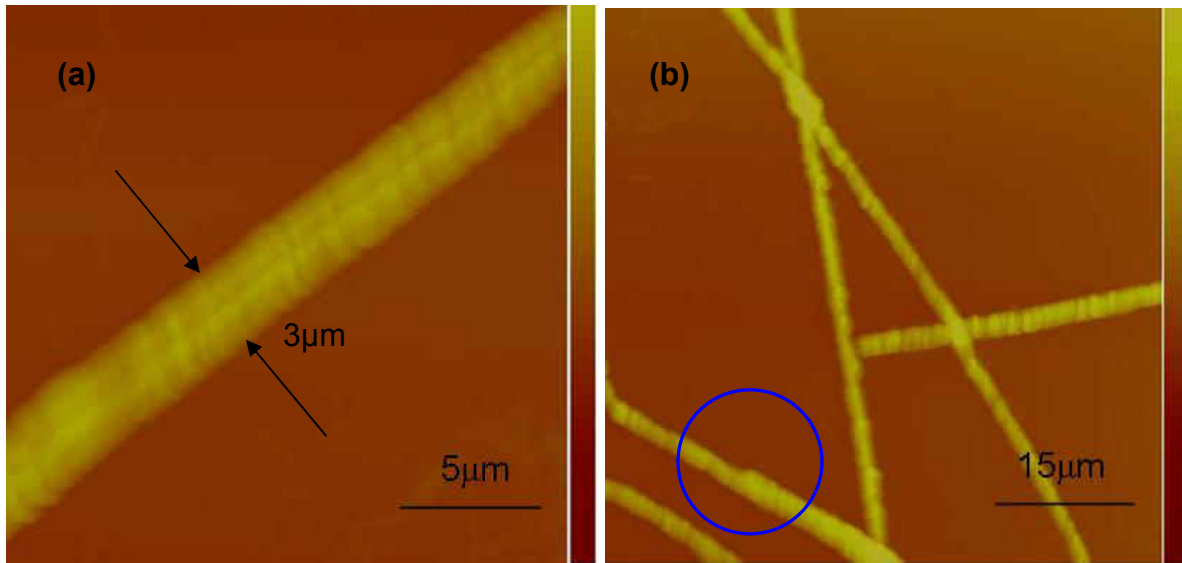


Figure 2.29 - AFM images of EDA sample (a) Showing fiber structure (b) Layered growth of fibers

EA sample

The ethylamine sample had faster kinetics compared to the EDA sample and formed aggregates in a shorter span of time. The aggregates looked like those found in the sodium lithocholate sample at low pH (about 7). The branched of the aggregates were seen to be quite straight but thin and the aggregate was dense.

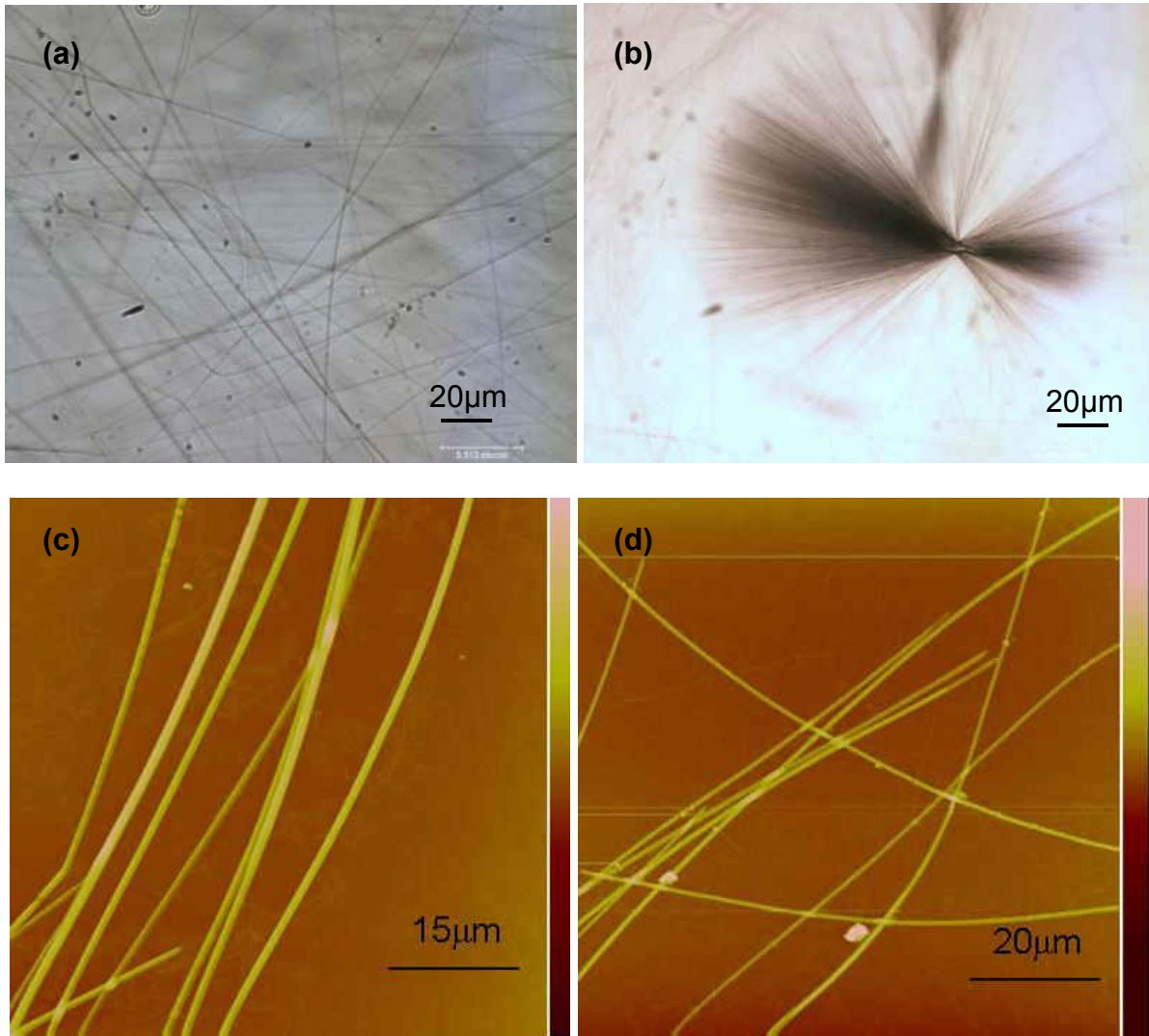


Figure 2.30 - EA sample (a) Individual fibers/tubes (b) Aggregation (c) & (d) AFM images

The structures look uniform with a smooth surface. It can be seen that the EA sample contains straighter tubes/fibers than the EDA sample. Though both can be considered straight structures, their degree of rigidity (or persistence length) is different. FTIR analysis of both samples [Fig. 2.30] shows results similar to those received for the SLC tubes/fibers.

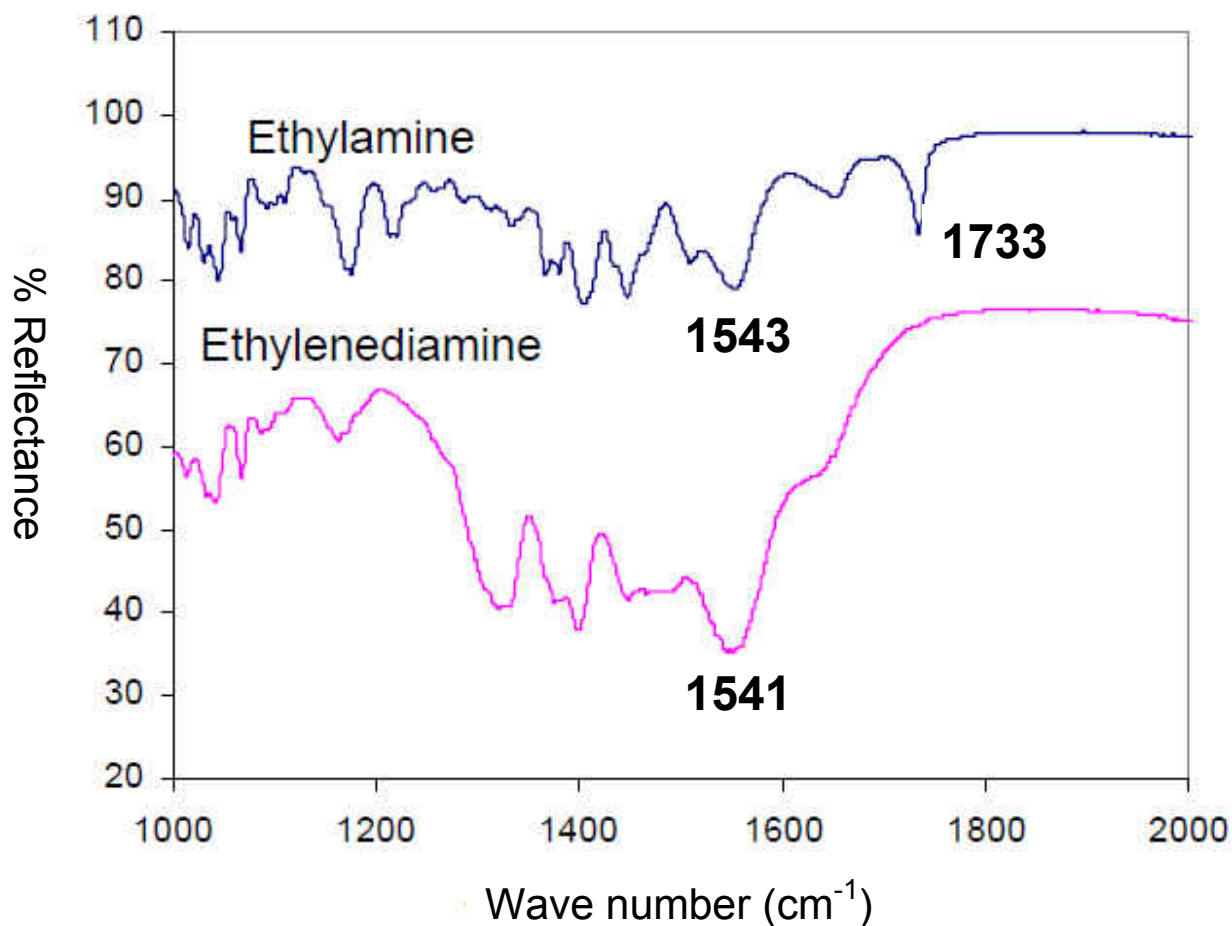


Figure 2.31 - FTIR studies of 0.1% w/w LCA samples with 0.1M EDA and EA

The most important peaks to consider are the one near 1550cm^{-1} and 1730cm^{-1} . As discussed in section 2.3.3, the peak at 1733cm^{-1} for the EA sample suggests that the LCA in that sample is partially deprotonated (unlike the EDA sample) and thus is more capable of hydrogen bond formation. Consequently, the tubes/fibers found in the EA sample are straighter as seen in the optical microscope images.

CHAPTER 3: FORMATION OF LIQUID CRYSTALS

This chapter deals with the actual formation of the liquid crystalline phases using the self-assembled tubes in the synthesized sodium lithocholate samples. The ordering of the LC domains was seen to be dependent on various physical and chemical parameters associated with the self-assembling system. A variety of experiments were conducted in order to qualitatively study the formation of LC phases and their textures in different environments.

3.1 Mechanism of Formation of Liquid Crystals

. It has been demonstrated that a combination of secondary hydrogen bonding with coulombic forces of ionic amphiphiles can lead to liquid crystal formation ^[68]. As mentioned in earlier sections of the manuscript, the amphiphilic moieties we use are ionic and they exhibit hydrogen bonding as well. It is believed that the liquid crystalline phases are formed from the self-assembled structures described in chapter two. These LCs formed typically in the high LCA concentration samples i.e. in samples, containing 1-4% w/w LCA. The mesogen concentration is expected to be proportional to LCA concentration in the samples. A direct and concrete relation between the two concentrations, however, could not be established. At the mentioned LCA concentrations, the samples were thick, viscous solutions which appeared whitish translucent to the eye. The translucent character of the samples suggested that the entities dispersed in them were neither too large nor too small (of the order of individual molecules). On account of the high viscosity of the samples, it was speculated that the

growth rate of the small self-assembled mesogens, was extremely low as was confirmed by the fact that large aggregates were formed sooner in solutions of lower concentrations. The passage of adequately large periods of time, transformed these samples into white opaque materials too, announcing the formation of large aggregates. The ordering of above-said mesogens took place in a variety of conditions and is better described in subsequent sections of this manuscript.

3.2 Concentration-induced Liquid Crystal formation in Open Cells

Initial studies were carried out using open cells to view samples. The structure of these cells is shown in Fig. 3.1 below.

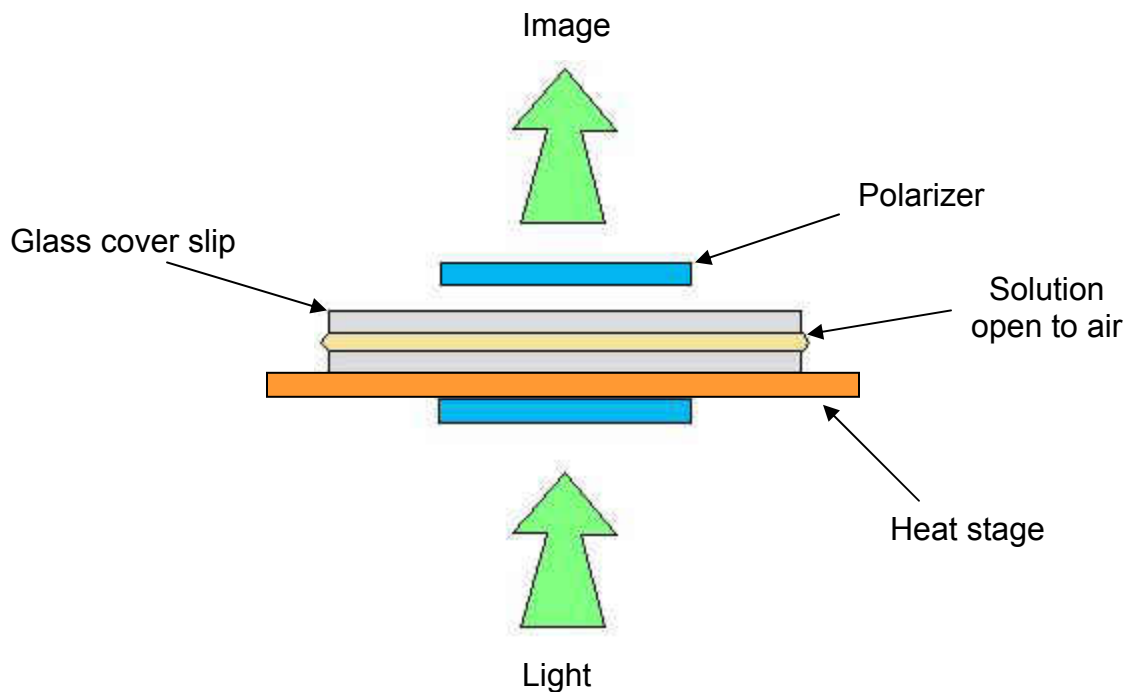


Figure 3.1 - Cross sectional view of an open cell

The open cell consisted of the solution or sample sandwiched between two glass cover slips. The solution was open to atmosphere from the sides as seen in the figure. The cell was heated on a heat stage and observed under an optical polarizing microscope. Let us introduce the general concept of the process used to obtain liquid crystals in this experiment.

3.2.1 Experimental Method

Solution of appropriate LCA concentration (1-4% w/w) was placed on the glass substrate and a second substrate was placed gently on top of the solution. The solution flowed and formed a thin film between the substrates. The volume of solution used was kept fixed to about 150 μ l in all experiments concerning open cells. The open cell was subsequently placed on a heat stage and heated in increments of 5 and 10°C to about 70°C while recording images at intermediate temperatures. Finally the heat stage was shut down to initiate rapid cooling of the cell to room temperature. In another set of experiments, the sample was directly heated to 70°C when the transition to isotropic phase took place, and the sample was kept in contact with the heat stage. It was brought into view over the viewing window so as to sever contact between the viewed region and the heat stage while the remaining cell area still maintained contact with the heat stage. The sample was allowed to stand in this condition at high temperature for a few minutes.

3.2.2 Results and Discussion

During the processes mentioned in the previous section, the sample was affected by three parameters, viz. change in concentration (through evaporation), flow due to

evaporation and change in temperature. It is a well-known fact that concentration of the amphiphiles is an important parameter that plays a role in the formation of LC phases in lyotropic systems. We also know that changes in temperature are equally important in bringing about LC transitions. Furthermore, flow-induced orientation of colloids is perhaps the oldest technique of establishing alignment in soft materials. By varying all three important parameters at once, we aimed to test the possibility of the formation of a liquid crystalline phase in the sample. The experiment was a success and liquid crystalline domains could be seen in samples of different LCA concentrations.

3.2.2.1 General Observations during Open Cell Thermal Processing

The behavior of all samples was similar during the open cell processing and hence, it is described in general for one of the samples viz. the one containing 2% w/w LCA. The concentrations of LCA in the samples were 0.75%, 1%, 2%, 3% and 4%. The two different methods of heating the samples described in the previous section yielded different textures of the LC phase. The texture observed on stepwise heating was coarser than the one observed on heating directly to a high temperature. It is thought that the coarse structures are formed as a result of less mobility on account of a high degree of evaporation (consequently increase in viscosity) during stepwise heating. This theory is also supported by the fact that the sample with the highest concentration of LCA (4% w/w) always showed coarse domains on account of high viscosity. Moreover, the 3% LCA sample showed coarse domains when heated stepwise but showed fine, small domains on direct heating. However, the final comparison is not conclusive enough evidence since the comparison was not made on the same day. Typical coarse

domain structure can be seen from the 4% LCA sample heated stepwise on day 2 after synthesis [Fig. 3.2]

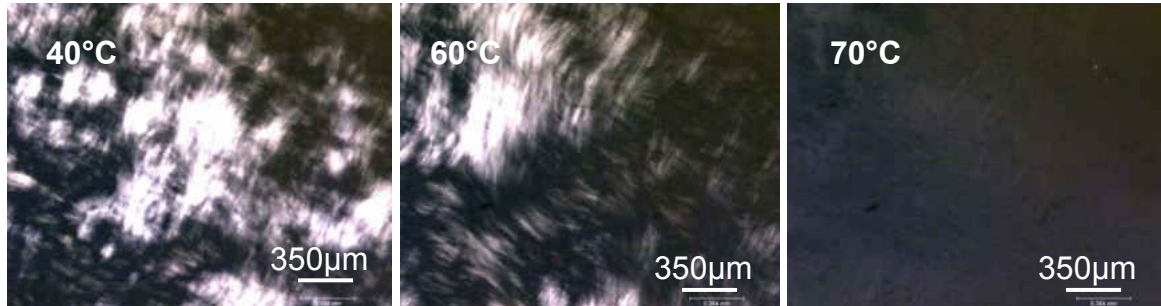


Figure 3.2 - Stepwise heating of 4% LCA sample in open cell

The images recorded during the subsequent cooling of the 4% LCA sample are displayed in Fig. 3.3. The observed domains had a striped texture which suggests the presence of cholesteric liquid crystalline phase.

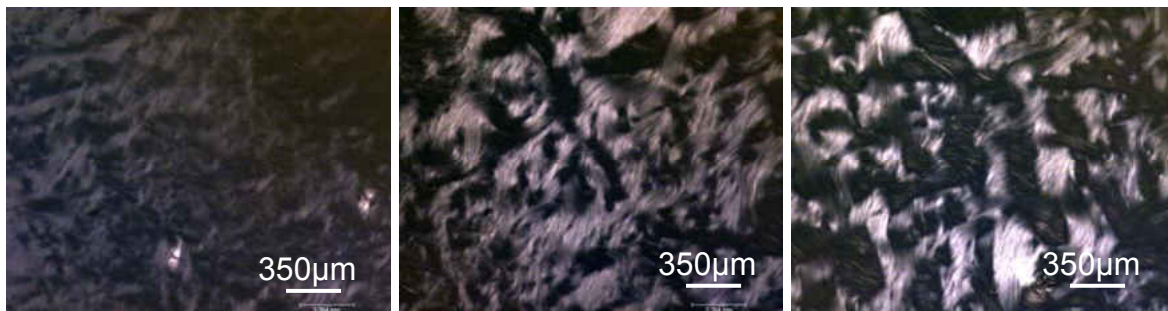


Figure 3.3 - Cooling of 4% LCA sample in open cell (from Fig. 3.2)

The domains were seen to grow as time progressed and they transformed into finer structures i.e. their texture became finely striped [Fig. 3.4]. This is thought to happen on account of better packing of the fibers in the domains.

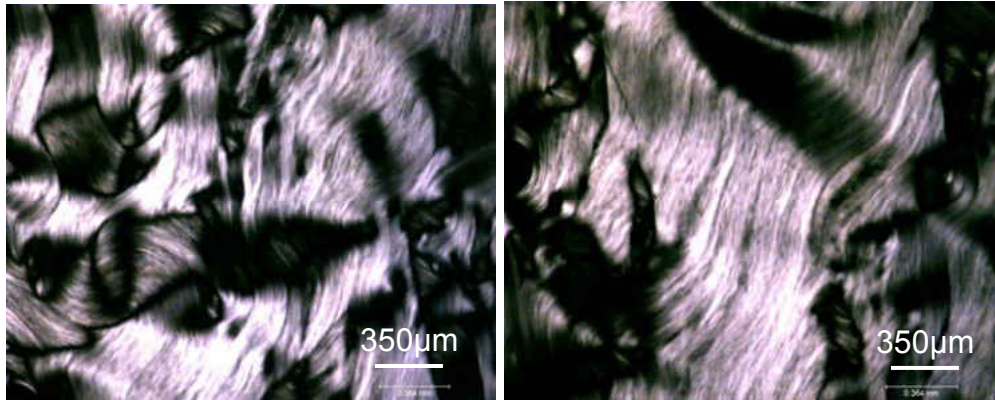


Figure 3.4 - Growth of coarse LC domains with time (from Fig. 3.3)

In the experiments where the sample was directly heated to 70°C and kept over the viewing window for a while, finer structures were obtained and this is illustrated by the series of images obtained for the 3% LCA sample (day 5). The temperature of the heat stage was maintained at 70°C throughout the process. However, the temperature of that part of the cell which was above the viewing window was bound to be lower due to absence of contact between the cell and the stage. Thus, technically the temperature of the region being viewed reduced below the transition temperature (70°C) when it was allowed to stand for a while and the transition occurred.

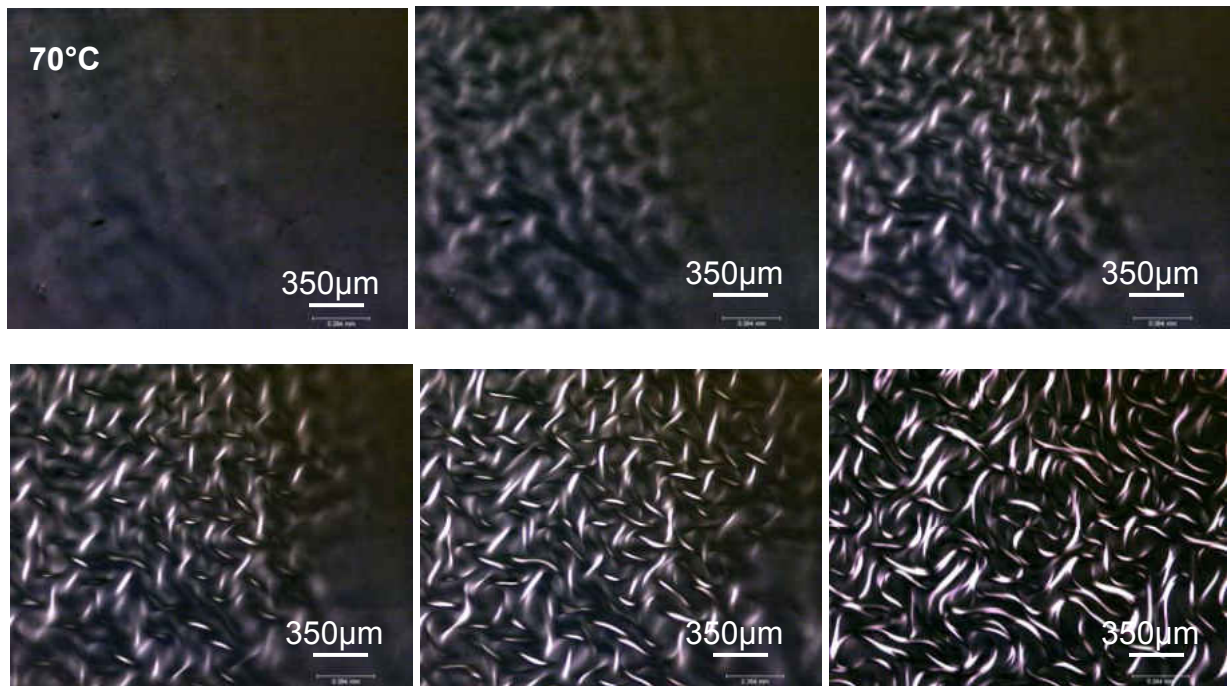


Figure 3.5 - Formation of fine domains through direct heating of 3% LCA sample on cooling

The mesogens (aggregates of extremely thin fibers) are visible if a bright field image is recorded after cooling the sample. It was also noted that even the fine domains grew with time to form ribbon-like domains after a few hours of standing at room temperature. This is illustrated by the images in the figure below.

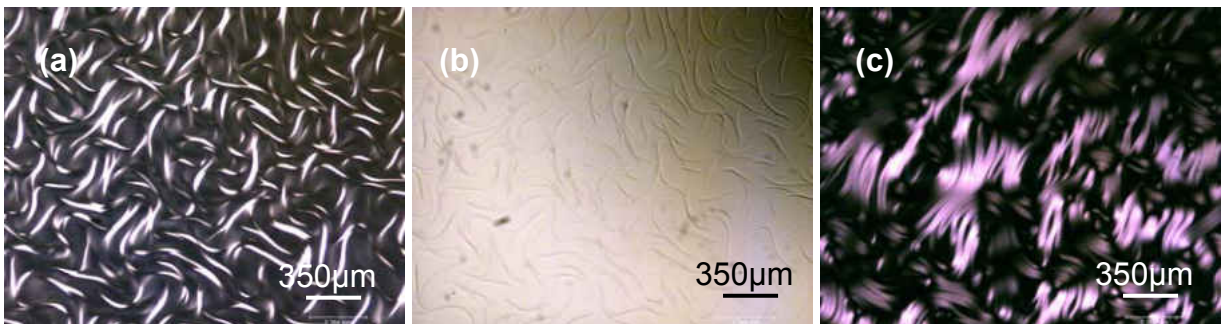


Figure 3.6 - 3% LCA sample (a) Dark field image when cooled after direct heating (b)

Corresponding bright field image (c) Growth of domains with time

3.2.2.2 Concentration dependence of LC phases

The self-assembly process is seen to be concentration dependent and, consequently, so is the process of liquid crystal formation. Thus in the initial stages of self-assembly, the number of fibers formed in the samples with lower LCA concentration is not enough to generate an LC phase as seen from Fig. 3.7. Only samples with 3% w/w LCA and above show some domain formation. Although it can be seen that the nature of the pattern formed on cooling progressively improves with increasing LCA concentration.

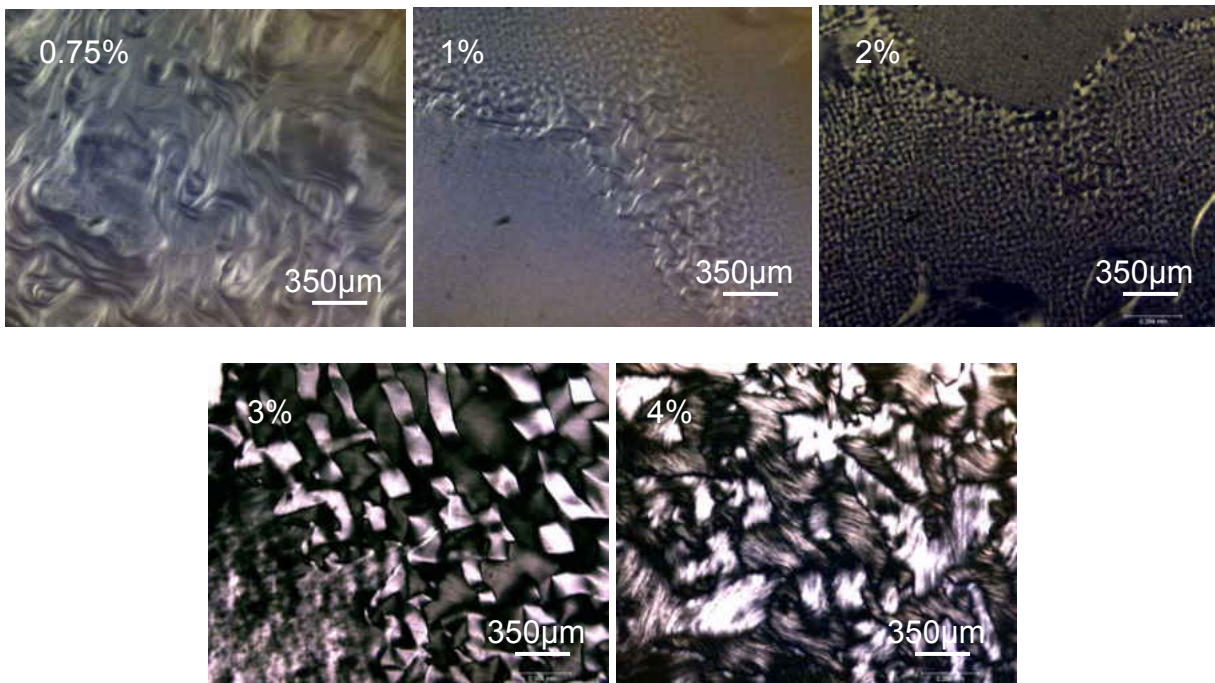


Figure 3.7 - Change in optical pattern with respect to LCA concentration

The 3% LCA sample forms domains only near the edge while the interior of the sample is in a disordered state.

3.2.2.3 Time dependence of LC phases

As seen in the above experiments, the liquid crystal phases form better in samples having more amounts of LCA since more self-assembled structures are formed quickly. Similarly, there is an increase in the number of fibers in all samples as time progresses. Hence, samples that initially do not show formation of LC phases do so after a certain period of time when the concentration of mesogens in the sample apparently reaches a sufficient value. Again, it is hard to gauge the exact progress of this concentration increase since we do not know the exact relation between LCA concentration and fiber concentration. However, it is quite clear from previous discussions in this thesis that the number of self-assembled structures increases in the samples with time. It is, thus, safe to create a notion that in all cases, the concentration of mesogens is proportional to both, LCA concentration as well as time. Fig. 3.8 depicts the progress of pattern development of a sample with time.

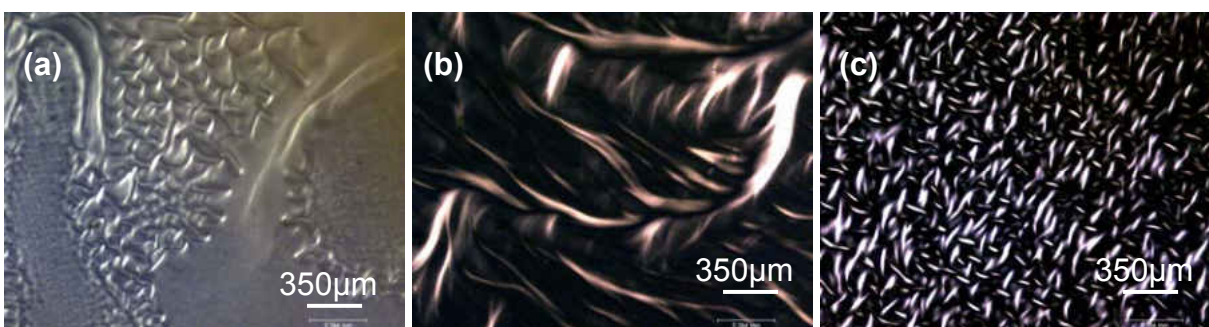


Figure 3.8 - Temporal progress of 1% w/w LCA sample with respect to LC formation (a) Day1

(b) Day 2 (c) Day 5

As seen above, on day 1 the sample showed isolated patches of crude patterns that displayed weak birefringence. Day 2 showed a higher degree of arrangement in

comparison but day 5 showed perfectly uniform and well-defined domains in the sample. All the images were recorded after cooling the samples to room temperature.

3.2.2.4 Evaporation induced LC phase formation in absence of heating

In previous discussions we have talked about the experimental procedure for the formation of liquid crystals in an open cell. In this procedure, the sample was affected by three variables viz. concentration, temperature and flow. Since the cell is open, evaporation and flow are bound to take place and hence to exclude the effect of temperature, a 2%w/w LCA sample was allowed to stand in a cell at room temperature to observe if liquid crystalline phase formed only due to the increase in concentration. It is possible to use evaporation and flow to give rise to LC phases in the sample. As the evaporation proceeds, flow occurs, pushing the liquid toward the edges and increasing the local concentration to a large extent. This causes the mesogens to align and show the appearance of a liquid crystalline phase.



Figure 3.9 - Evaporation induced LC formation (a) Initial stage (b) Ordering at the edge (c) Growth of domains with time

This set of experiments suggested that the liquid crystalline materials formed at a higher concentration of LCA than the samples were made out of. However, this was fairly easy to achieve through evaporation.

3.2.2.5 Effect of pH on LC formation

Earlier in this document we have come across the phenomenon of morphology change based on pH values. We tried to employ this concept to form different mesogens and thus, achieve a different mesophase. The fibers broke into shorter ones as expected when the pH was lowered to between 7 and 8. These fibers aligned themselves in a manner different than what had been seen in the high pH samples. The fibers seemed to be aligned in the same general direction as in a nematic mesophase [Fig. 3.10].

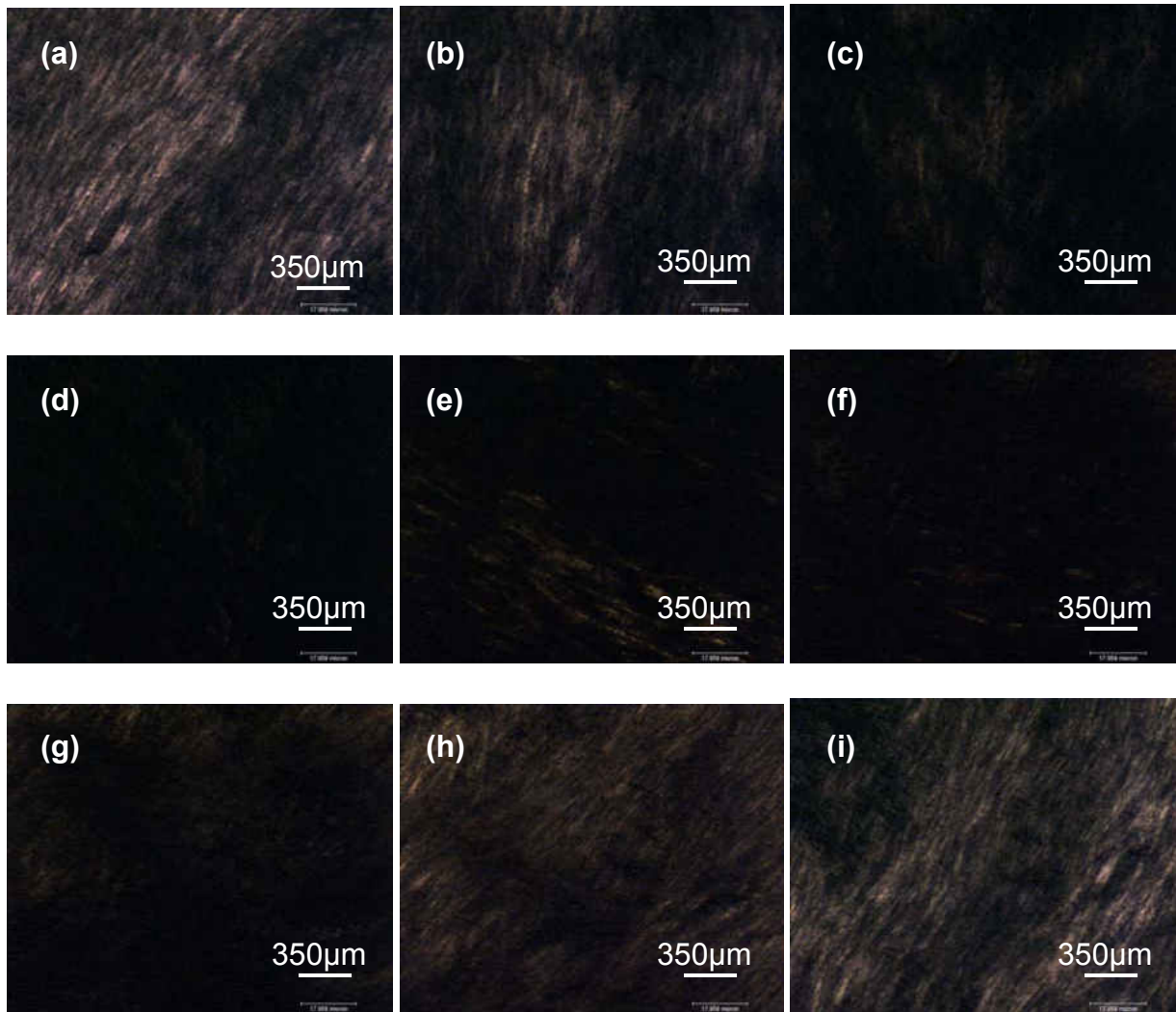


Figure 3.10 - 2% w/w LCA sample at near neutral pH

Fig. 3.10 (a) to (i) depict the birefringence shown by the sample on rotation through 180° . This confirms the nematic nature of the liquid crystalline phase observed.

3.3 Temperature-induced Liquid Crystal formation in Closed Cells

3.3.1 Plain Glass Cells

In order to investigate the possibility of liquid crystal formation due to the temperature alone, the same heat treatment was given to the sodium lithocholate samples after they were enclosed in glass cells. This limited evaporation and thus, kept the LCA concentration constant throughout the span of the experiment. The setup is illustrated below in Fig. 3.11.

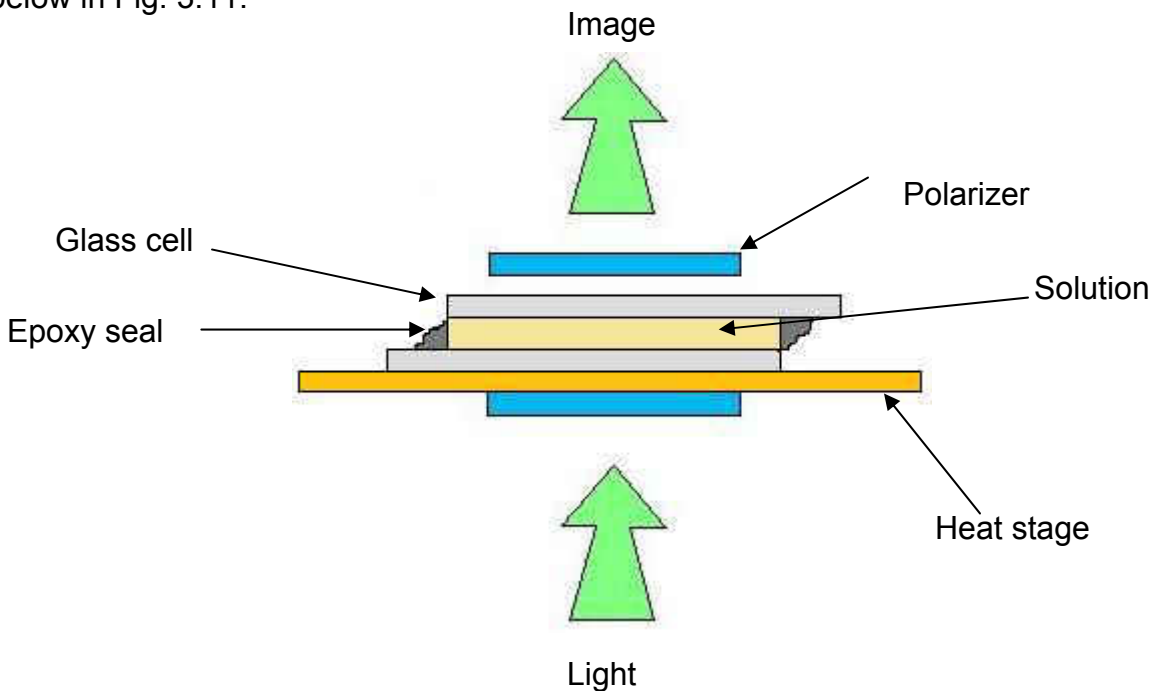


Figure 3.11 – Cross sectional view of a closed cell

The sample was enclosed in a cell made of glass slides of 1mm thickness with 200 μ m thick spacers between them. The cell was then sealed with epoxy so as to avoid evaporation of the solution. Finally it was heated to 75°C directly and observed under a

polarizing optical microscope. The initial pattern melted away as usual into an isotropic phase and on cooling, rough domains were seen to form.

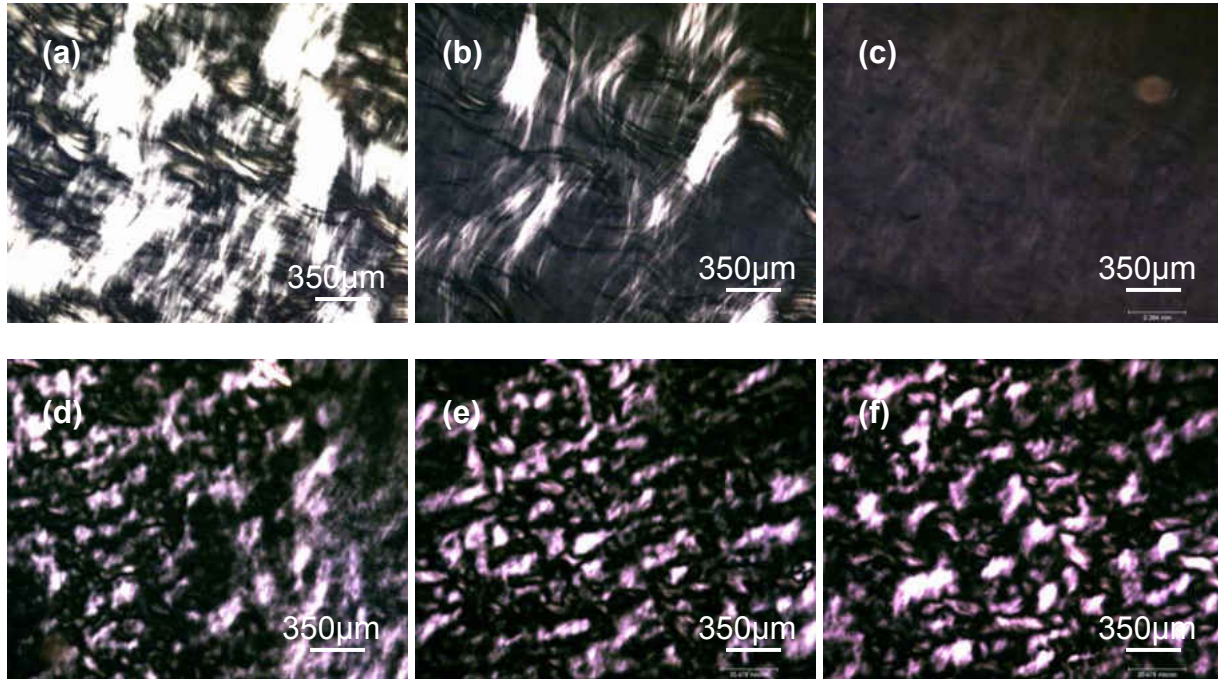


Figure 3.12 - 3% w/w LCA sample in a closed cell

Parts (a) (b) and (c) of Fig. 3.12 show changes in the sample as it was heated from room temperature to 75°C while parts (d) (e) and (f) show the rough domains that were observed after the sample was cooled down to room temperature again. The observed domains were not as good as those seen before and it was thought that evaporation to a large extent was essential for the LC phase to form. But when the sample was viewed again after a time span of about 24 hours, the domains had acquired stripes which are characteristic of cholesteric liquid crystalline phases [Fig. 3.13].

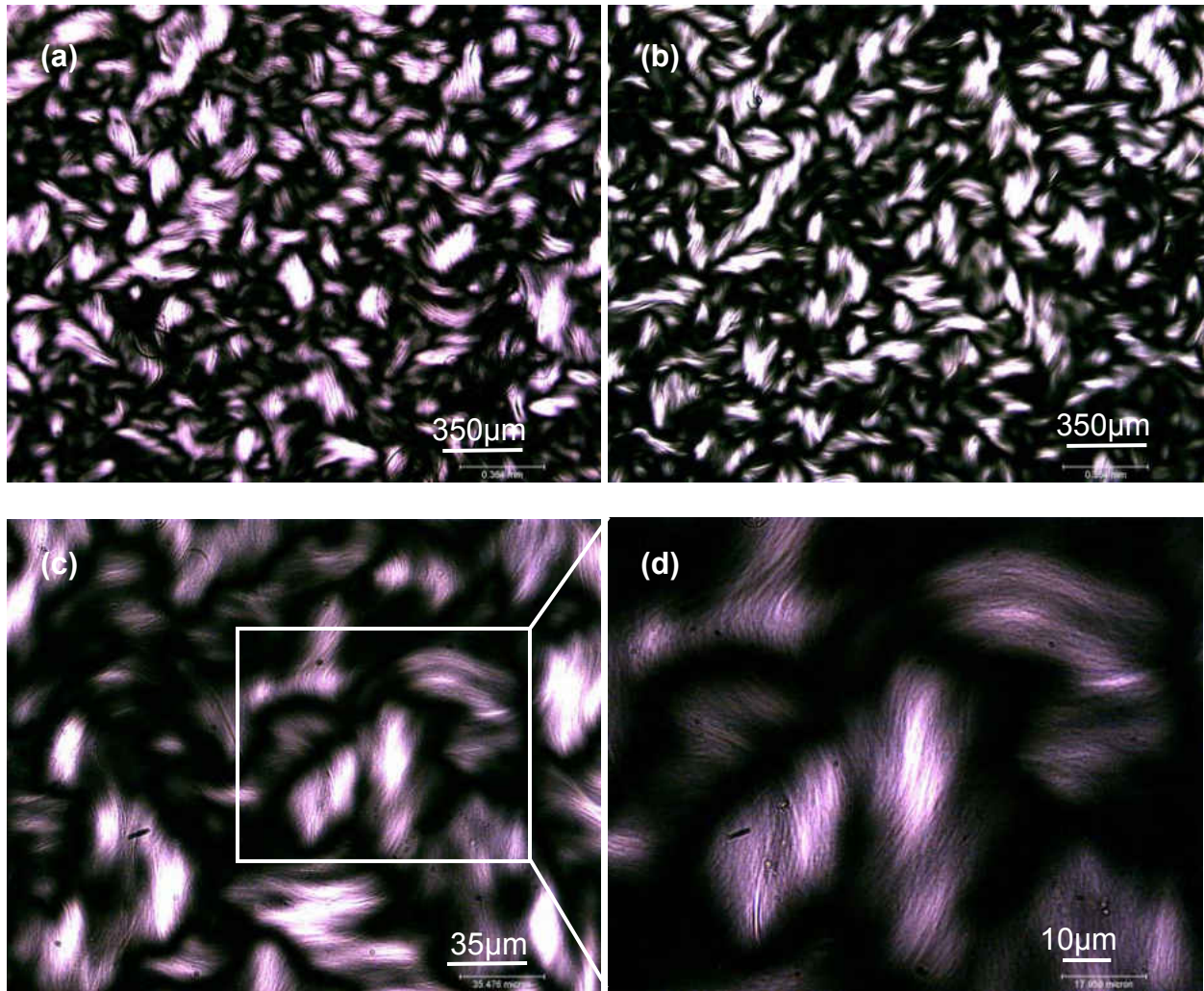


Figure 3.13 - Cholesteric LC phase in 3% w/w LCA sample

In the above images, parts (c) and (d) show the striped structure of the domains quite clearly. All the images are dark field polarizing microscope images taken at different magnifications.

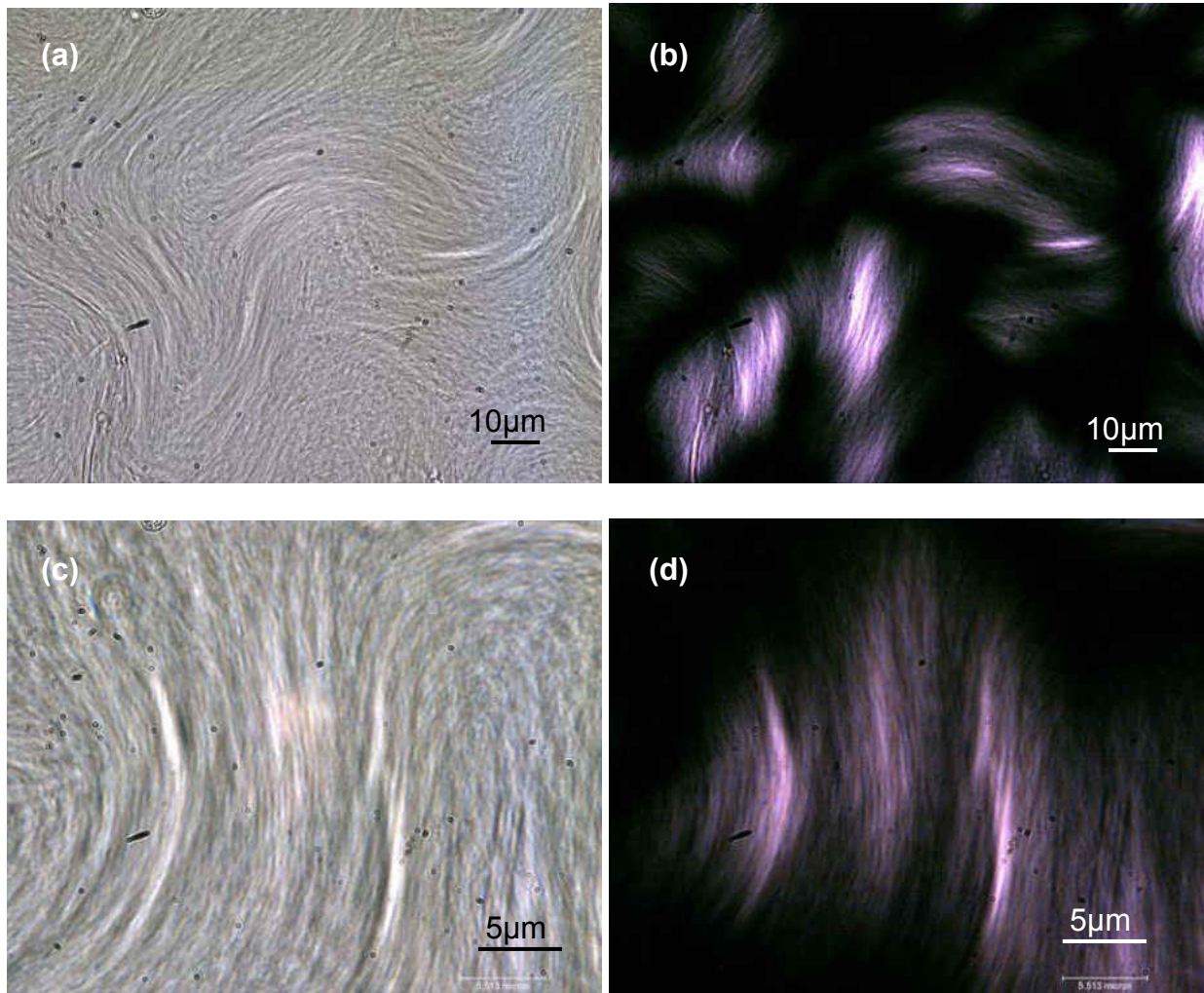


Figure 3.14 - Image showing fiber arrangement in 3% w/w LCA sample

The orientation of the fibers decides the brightness of the corresponding part of the dark field image. Fig. 3.14 (a) & (c) show optical images of the sample while Fig. 3.13 (b) & (d) show their corresponding dark field images. It can be clearly seen that when the orientation of the fibers is roughly around 45° to the horizontal, or when there is no preferred orientation, the image shows dark spots. This experiment proves that temperature can trigger the formation of liquid crystals as well, though this process is much slower in comparison to the method using evaporation.

3.3.2 Glass Cells Coated with Polyimide Layer

In order to study the effect of alignment layers on the LC phases formed from our samples, they were introduced into cells having an interior coating of parallel polyimide layers. The phases were seen to align slightly better than they did in the absence of the polymer layers. The domains observed were longer than usual and their length seemed to increase in the direction of polymer alignment. As the thickness of the cells increased, the samples exhibited stronger birefringence, suggesting that the LCs exist as layered structures.

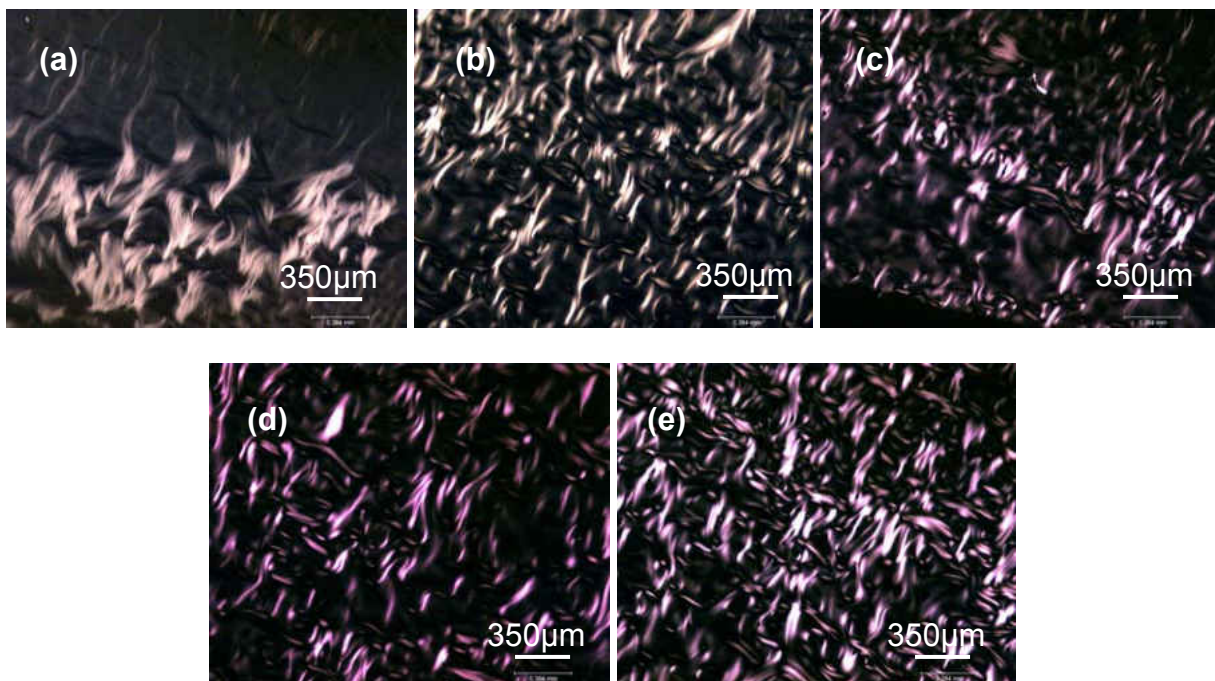


Figure 3.15 - LC alignment in polymer coated cells with respect to cell thickness (a) 5 μ m (b) 8 μ m (c) 10 μ m (d) 12 μ m (e) 15 μ m

With increasing cell thickness, the samples were seen to resemble LCs formed in the thick cells. This was expected since with increase in cell thickness, the influence of the polymer layer on the mesogens, decreases.

3.3.3 Liquid Crystals in a Channel

Lastly, the effect of flow on ordering was studied by confining the 2% w/w LCA sample in a microchannel and then making it flow by application of pressure.

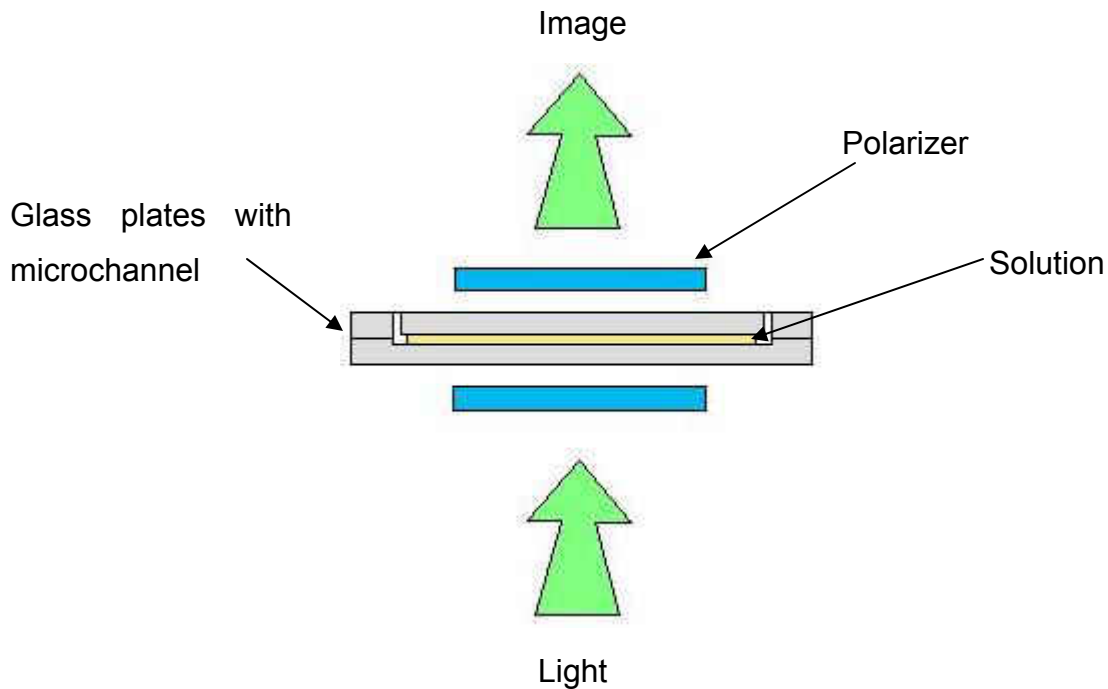


Figure 3.16 - Liquid Crystal formation in a microchannel

The sample was introduced into the channel and then heated in an oven to 75°C for ten minutes. The evaporation was assumed to be negligible since the channel openings were sealed with tape. The sample was removed from the oven and directly viewed under the microscope. The sample showed increased birefringence as it cooled down, indicating definite ordering.

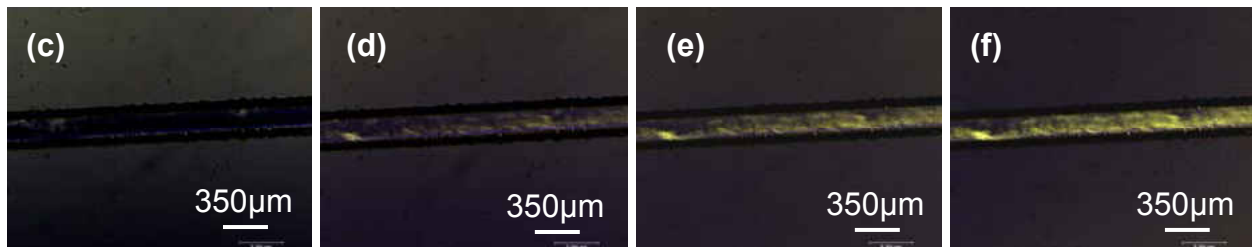
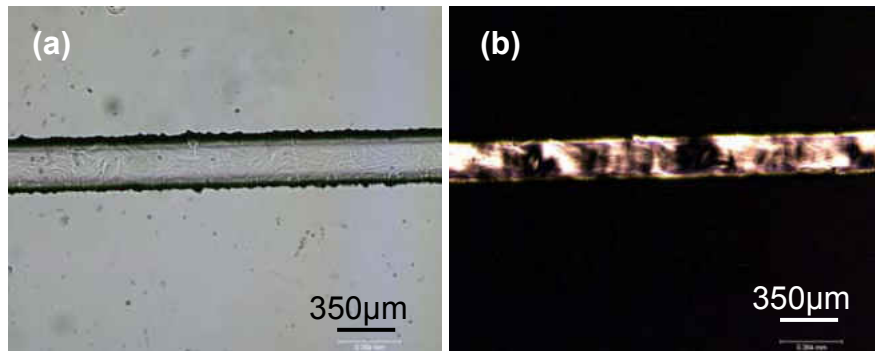


Figure 3.17 – 2% w/w sample (a) & (b) Disorder before heating (c) to (f) Ordering during cooling

Moreover, when the channel was rotated under the cross polarizers, it was seen that the phase formed, was a nematic LC phase.

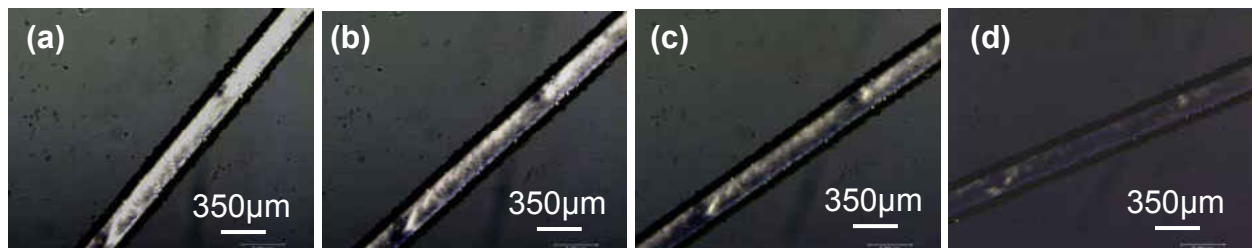


Figure 3.18 - Nematic phase observed in the channel (clockwise rotation)

On subjecting the sample to flow, it was apparent that rearrangement of mesogens took place giving rise to ring-like domains in the channel. These domains resembled parabolic velocity profiles, so often seen during laminar flow of fluids through channels.

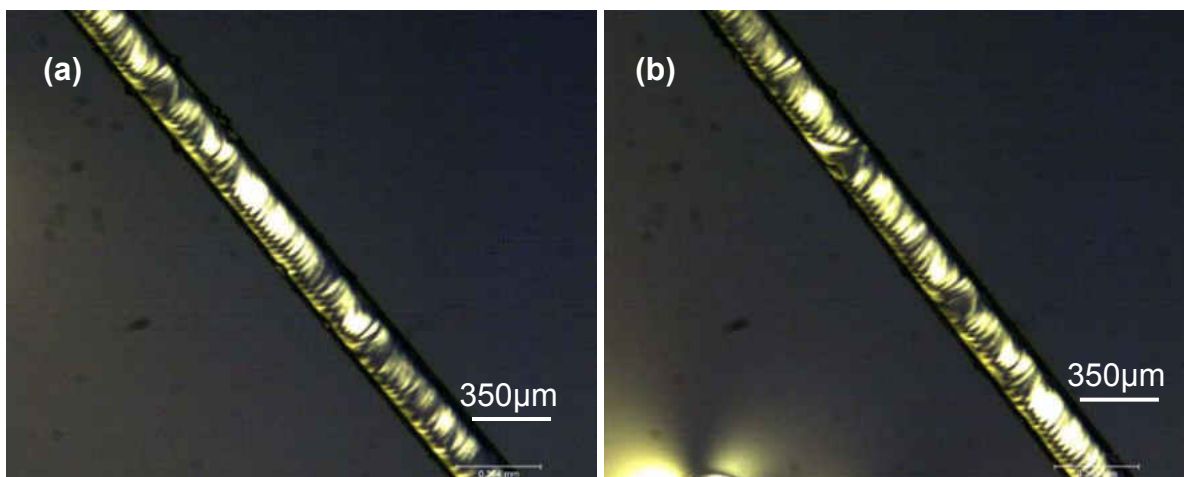


Figure 3.19 - Rings formed in the channel due to flow

3.4 Formation of LC Phases from EA and EDA samples

As seen in chapter 2, LCA molecules self-assemble in the presence of organic bases like ethylamine (EA) and ethylenediamine (EDA) to give fibers and tubes. Since LCA solutions containing these bases form self-assembled structures, it was thought to make use of these structures to form liquid crystalline materials as well. 2% w/w LCA samples were made using the usual procedure of adding LCA to 0.1M aqueous basic solution. It was observed that since EDA had more affinity towards water (EDA samples are very hard to dry) it formed much better LC phases than the EA sample which dried up quickly. The samples were viewed inside closed glass cells with 200µm spacers.

3.4.1 LCA with Ethylamine

The EA sample was introduced into a closed cell and heated in steps from 40°C to 65°C in increments of 5°C.

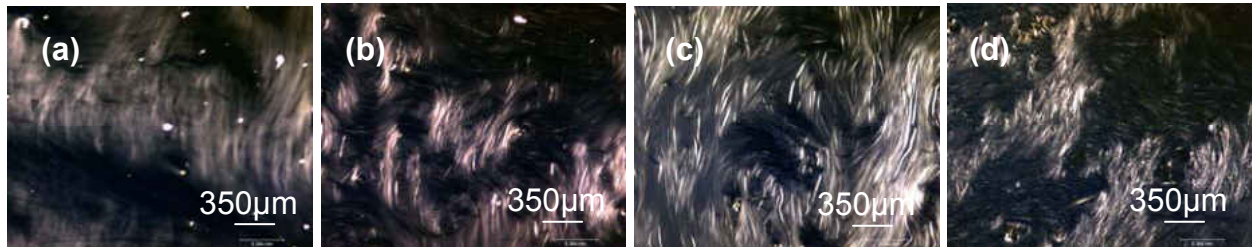


Figure 3.20 - 2% w/w LCA in EA solution (a) 40°C (b) 50°C (c) 60°C (d) 65°C

The rate of self-assembly of LCA in EA is very high and large aggregates are formed rapidly irrespective of concentration. It is seen that instead of arranging in domains, the EA sample prefers to form thicker fibers by the end of the heating cycle. Hence the idea of using EA to form liquid crystals is abandoned.

3.4.2 LCA with Ethylenediamine

The EDA sample was treated to the same heating process described in the previous section. However, the changes that were observed in this sample were quite different. The sample underwent a transition to the isotropic phase as in the case of SLC samples. The transition temperature was 65°C in this case which was lower than that seen in SLC samples.

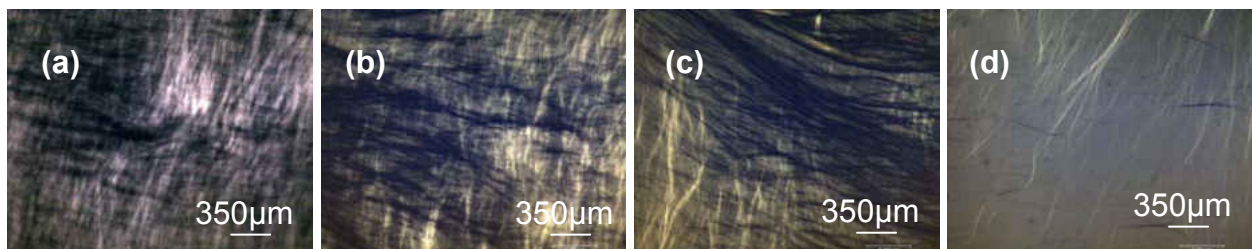


Figure 3.21 - 2% w/w LCA in EDA solution (a) 40°C (b) 50°C (c) 60°C (d) 65°C

On keeping the sample in the viewing window, the temperature reduces slightly as is explained in section 3.2.2.1 and the isotropic – liquid crystalline phase transition occurs.

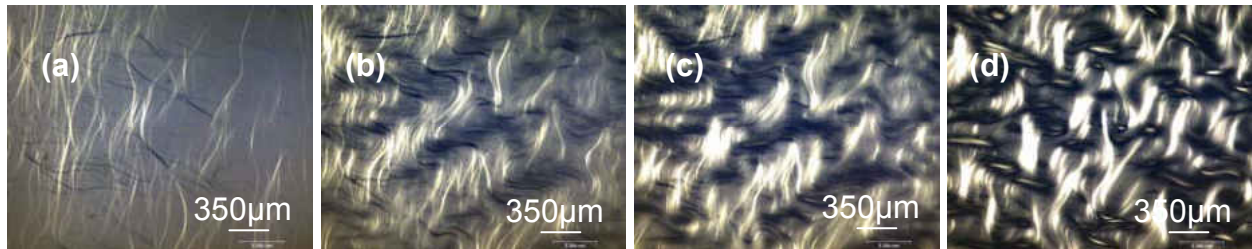


Figure 3.22 - Formation of LC phase in EDA sample

On viewing the sample after 2 hours, the domains were seen to grow as expected and the ribbon-like domains were seen [Fig. 3.23].

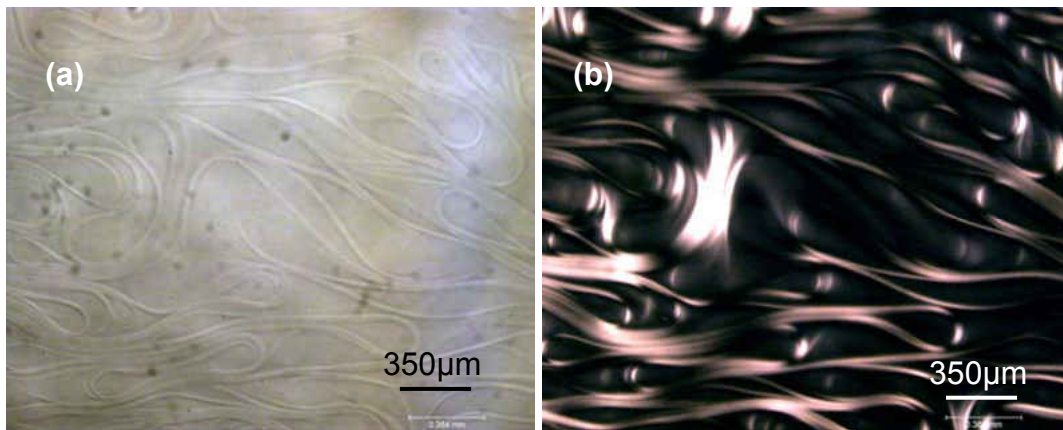


Figure 3.23 - 2% LCA with EDA sample after 2 hours (a) Bright field image (b) Dark field image

The EDA sample is thus a good choice as a raw material for the synthesis of LC phases

CHAPTER 4: CONCLUSION

This thesis can be divided into two main sections viz. the self-assembly of LCA and the organization of these self-assembled structures into LC phases. The process of self-organization of naturally occurring bile acid molecules in alkaline aqueous solutions under a range of experimental conditions using a variety of materials was investigated and documented. The study of self-assembly and its sensitivity to experimental conditions and environments has led to the concept of controlled synthesis of supramolecular structures with a defined set of properties. The effect of parameters like concentration, temperature, pH, etc. on the process as well as the products of LCA self-assembly has been documented in this thesis. We have described the synthesis of self-assembled structures with various shapes and morphologies depending on the base conjugated with LCA. AFM studies were carried out on all samples to provide information regarding the size and morphology of the assemblies in the various samples synthesized. FTIR spectroscopy was employed to understand the molecular interactions involved in the change in properties of the supramolecular assemblies at different experimental conditions. Polarizing optical microscopy was used to observe the progressive aggregation of the LCA structures as well as record the birefringence properties of the aggregates. It was observed that the increase in concentration and temperature above a certain level led to the formation of gel-like materials instead of individual tubes or aggregates. The control of sample pH was seen to be the simplest technique to control the shape of the self-assembled structures.

A thorough study of the processes and conditions required to produce special materials is a prerequisite to their large scale synthesis and subsequent application. This thesis delves into these aspects in order to establish a foundation for further investigation. It shows for the first time that supramolecular assemblies made of biological molecules can be used as precursors for liquid crystal formation. It describes different methods of obtaining LC phases through the use of various driving forces like temperature, concentration and shear. It provides a multitude of ways by which to form liquid crystalline phases from the self-assembled supramolecular structures viz. by using open cells, closed cells and channels. The optical textures of the LC phases were recorded using a polarizing microscope. Cholesteric and nematic liquid crystals were seen to form in flexible and rigid fiber samples. The optimum LCA concentration for LC formation was seen to be in the range of 2% - 4% w/w. The transition temperature for LC formation was noted to be about 70°C except in rare cases. Since the LC phases form from self-assembled precursors, the LC formation is also time dependent. The change in physical parameters of the liquid crystal cells did not affect the transition temperature significantly. A marginal increase in alignment of the samples was observed in cells coated with polyimide. Liquid crystalline phases were obtained in all samples with LCA concentration above 0.75% w/w. The mesophases are believed to be formed from self assembled fibers and tubes since lyotropic liquid crystals always form through aggregation and observations in this study show that during the initial period of self-assembly, LC phases are not prominent. This study establishes the procedures and conditions required to synthesize self-assembled precursors for liquid crystal formation and describes methods to achieve LC phases in numerous ways. It also characterizes

the self-assembled structures and identifies the LC phases they form and is thus, a complete qualitative study of the process of formation of lyotropic liquid crystals through the self-assembly of bile acid building blocks.

LIST OF REFERENCES

1. M. Bruchez Jr., M. Moronne, P. Gin, S. Weiss, A. P. Alivisatos; *Science*, **1998**, *281*, p2013.
2. N. C. Seeman; *Biochem.*, **2003**, *42*, p7259
3. M. A. Haque and M. T. A. Saif; *J. Microelectromech. Sys.* **2001**, *10*, p146.
4. J. E. Mark; *Poly. Eng. Sci.*, **1996**, *36*, p2905.
5. Markus Heim, David Keerl, and Thomas Scheibel; *Angewandte Chemie*, **2009**, *48*, p3584.
6. Natalio Krasnogor, Steve Gustafson, David A. Pelta and Jose L. Verdegay, Eds; *Self-Assembly: Multidisciplinary Snapshots*, **2008**, Elsevier Science.
7. A. R. Hemsley, M. E. Collinson, W. L. Kovach, B. Vincent and T. Williams; *Phil. Transac. Bio. Sci.*, **1994**, *345*, p163.
8. Scott Camazine, Jean-Louis Deneubourg, Nigel R. Franks, James Sneyd, Guy Theraulaz and Eric Bonabeau; *Self-Organization in Biological Systems*, **2003**, Princeton University Press.
9. George M. Whitesides and Mila Boncheva; *Proc. Natl. Acad. Sci.*, **2002**, *99*, p4769.
10. Ned B. Bowden, Marcus Weck, Insung S. Choi and George M. Whitesides; *Acc. Chem. Res.*, **2001**, *34*, p231.
11. D. Chapman; *Ann. NY Acad. Sci.*, **1966**, *137*, p745.
12. F. Reinitzer; *Montasch Chem.*, **1988**, *9*, p421.
13. O. Lehmann; *Zeitschrift für Physikalische Chemie*, **1889**, *4*, p462.
14. G. Friedel; *Ann. Physique*, **1922**, *18*, p273.
15. S. Chandrasekhar; *Liquid Crystals*, **1930**, Cambridge University Press.

16. Peter Collings and Micheal Hird; *Introduction to liquid crystals chemistry and physics*, **1997**, Taylor & Francis.
17. S. Chandrasekhar and N. V. Madhusudana; *Ann. Rev. Mater. Sci.*, **1980**, *10*, p133.
18. Iam-Choon Khoo and Shin-Tson Wu; *Optics and nonlinear optics of liquid crystals*, **1993**, World Scientific Publishing Company.
19. A. D. Buckingham, G. P. Ceasar and M. B. Dunn; *Chem. Phys. Letters*, **1969**, *3*, p540.
20. Birendra Bahadur; *Liquid Crystals Applications and Uses – Vol. 1*, **1990**, World Scientific Publishing Company.
21. Birendra Bahadur; *Liquid Crystals Applications and Uses – Vol. 3*, **1992**, World Scientific Publishing Company.
22. V. Luzzati and A. Tardieu; *Ann. Rev. of Phys. Chem.*, **1974**, *25*, p79.
23. Stig Friberg; *Naturwissenschaften*, **1977**, *64*, p612.
24. J. Israelachvili; *Intermolecular & Surface Forces.*, **1992**, Academic Press.
25. Peter Collings and Jay S. Patel, Eds.; *Handbook of Liquid Crystal Research*, **1997**, Oxford University Press.
26. D. Chapman; *Faraday Soc. Symp.*, **1971**, *5*, p163.
27. Patrick Oswald and Pawel Pieranski; *Nematic and cholesteric liquid crystals*, **2005**, Taylor & Francis.
28. Takashi Kato; *Science*, **2002**, *295*, p2414.
29. George Whitesides and Bartosz Grzybowski; *Science*, **2002**, *295*, p2418.
30. D. G. Oakenfull and L. R. Fisher; *J. Phys. Chem.*, **1977**, *81*, p1838.

31. P. Venkatesan, Y. Cheng, D. Kahne; *J. Am. Chem. Soc.* **1994**, *116*, p6955.
32. T. Shimizu, M. Masuda, H. Minamikawa; *Chem. Rev.* **2005**, *105*, p1401.
33. J. Y. Fang; *J. Mater. Chem.* **2007**, *17*, p3479.
34. A. Brizard, R. Oda and I. Huc; *Top. Curr. Chem.* **2005**, *256*, p167.
35. Shuguang Zhang; *Nat. Biotech.*, **2003**, *21*, p1171.
36. Yevgeniya V. Zastavker, Neer Asherie, Aleksey Lomakin, Jayanti Pande, Joanne M. Donovan, Joel M. Schnur and George B. Benedek; *Proc. Natl. Acad. Sci.*, **1999**, *96*, p7883.
37. Sylvain Vauthey, Steve Santoso, Haiyan Gong, Nicki Watson and Shuguang Zhang; *Proc. Natl. Acad. Sci.*, **2002**, *99*, p5355.
38. Shuguang Zhang, Davide M. Marini, Wonmuk Hwang and Steve Santoso; *Curr. Op. Chem. Bio.*, **2002**, *6*, p865.
39. Ned B. Bowden, Marcus Weck, Insung S. Choi and George M. Whitesides; *Acc. Chem. Res.*, **2001**, *34*, p231.
40. Davide M. Marini, Wonmuk Hwang, Douglas A. Lauffenburger, Shuguang Zhang and Roger D. Kamm; *Nano Lett.*, **2002**, *2*, p295.
41. Amilie Leforestier and FranQoise Livolant; *Biophysical Journal*; *65* (1993); 56-72.
42. Takashi Kato, Toru Matsuoka, Masayuki Nishii, Yuko Kamikawa, Kiyoshi Kanie, Tatsuya Nishimura, Eiji Yashima and Seiji Ujiie; *Angewandte Chemie*, **2004**, *116*, p2003.
43. Erik Winfree, Furong Liu, Lisa A. Wenzler and Nadrian C. Seeman; *Nature*, **1998**, *394*, p539.

44. G Zanchetta, M Nakata, M Buscaglia, N A Clark and T. Bellini; *J. Phys.: Condens. Matter*, **2008**, *20*, p494214.
45. H. H. Strey, J. Wang, R. Podgornik, A. Rupprecht, L. Yu, V. A. Parsegian, and E. B. Sirota; *Phys. Rev. Lett.*, **2000**, *84*, p3105.
46. K. Kassapidou, W. Jesse, J. A. P. P. Var Dijk, J. R. C. van der Maarel; *Biopolymers*, **1998**, *46*, p31.
47. Giuliano Zanchetta, Tommaso Bellini,, Michi Nakata, and Noel A. Clark; *J. Am. Chem. Soc.*, **2008**, *130*, p12864.
48. Alfons Enhsen, Werner Kramer and Günther Wess; *DDT*, **1998**, *3*, p409.
49. Ichiro Hisaki, Norimitsu Tohnai and Mikiji Miyata; *Chirality*, **2007**, *20*, p330.
50. D. M. Small, *The Bile Acids. Chemistry, Physiology and Metabolism - Vol. 1*; P. P. Nair, D. Kritchevsky, K. D. R. Setchell, Eds., **1971**, Plenum Press.
51. Martin C. Carey, Donald M. Small; *Arch. Intern. Med.*, **1972**, *130*, p506.
52. Funasaki, N.; Fukuba, M.; Kitagawa, T.; Nomura, M.; Ishikawa, S.; Hirota, S.; Neya, S. Two-dimensional NMR Study on the Structures of Micelles of Sodium Taurocholate. *J. Phys. Chem. B* **2004**, *108*, p438.
53. Y. Chen, J. Luo and X. X. Zhu; *J. Phys. Chem. B*, **2008**, *112*, p3402
54. L. B. Pártay, P. Jedlovszky and M. Sega; *J. Phys. Chem. B.*, **2007**, *111*, p9886.
55. Paula Messina, Marcela A. Morini, Pablo C. Schulz and Gerardo Ferrat; *Colloid Poly. Sci.*, **2002**, *280*, p328.
56. Aldo Roda, Alan F. Hofmann and Karol J. Mysels; *J. Bio. Chem.*, **1983**, *258*, p6362.

57. Ponnusamy Babu, Neralagatta M. Sangeetha, Uday Maitra; *Macromol. Symp.*, **2006**, 241, p61.
58. Elina Virtanen and Erkki Kolehmainen; *Eur. J. Org. Chem*, **2004**, 16, p3385.
59. Pierre Terech, Arnaud de Geyer, Bernd Struth and Yeshayahu Talmon; *Advanced Materials*, **2002**, 14, p495.
60. Mikiji Miyata, Norimitsu Tohnai, and Ichiro Hisaki; *Molecules*, **2007**, 12, 1973.
61. Shreedhar Bhat and Uday Maitra; *Tetrahedron*, **2007**, 63, p7309.
62. Bruno Jean, Liat Oss-Ronen, Pierre Terech and Yeshayahu Talmon; *Advanced Materials*, **2005**, 17, p728.
63. Niharendu Choudhury and B. Montgomery Pettitt; *J. Phys. Chem. B*, **2006**, 110, p8459.
64. Tuhin Ghosh, Amrit Kalra, and Shekhar Garde; *J. Phys. Chem. B*, **2005**, 109, p642.
65. Takatoshi Fujita, Hirofumi Watanabe, and Shigenori Tanaka; *Chem. Phys. Lett.* , **2007**, 434, p42.
66. Efrosini Kokkoli and Charles F. Zukoski; *Langmuir*, **1998**, 14, p1189.
67. Younghun Kim, Pil Kim, Changmook Kim and Jongheop Yi; *J. Mat. Chem.*, **2003**, 13, p2353.
68. Constantinos M. Paleos, Dimitris Tsiourvas; *Curr. Opin. Coll. Int. Sci.*, **2001**, 6, p257.